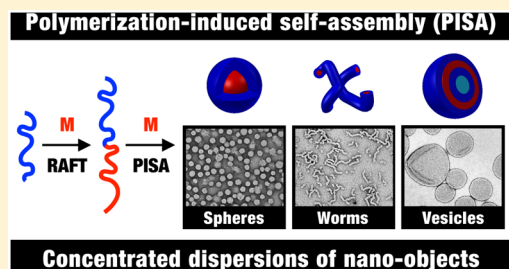


## A Critical Appraisal of RAFT-Mediated Polymerization-Induced Self-Assembly

Sarah L. Canning, Gregory N. Smith, and Steven P. Armes\*

Dainton Building, Department of Chemistry, University of Sheffield, Brook Hill, Sheffield, South Yorkshire S3 7HF, U.K.

**ABSTRACT:** Recently, polymerization-induced self-assembly (PISA) has become widely recognized as a robust and efficient route to produce block copolymer nanoparticles of controlled size, morphology, and surface chemistry. Several reviews of this field have been published since 2012, but a substantial number of new papers have been published in the last three years. In this Perspective, we provide a critical appraisal of the various advantages offered by this approach, while also pointing out some of its current drawbacks. Promising future research directions as well as remaining technical challenges and unresolved problems are briefly highlighted.



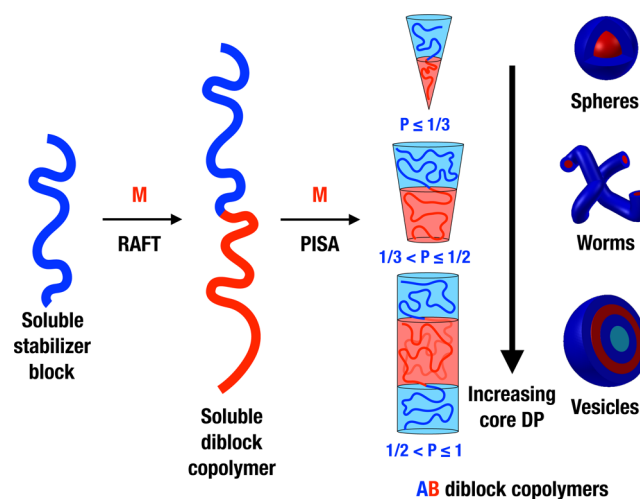
### INTRODUCTION

The self-assembly of surfactant amphiphiles has been studied for over 100 years;<sup>1</sup> McBain was the first to discuss the formation of micelles within soap solutions in 1913.<sup>2</sup> However, the study of block copolymer self-assembly only began in the early 1960s<sup>3–6</sup> following the discovery of living anionic polymerization by Szwarc et al., enabling access to well-defined block copolymers for the first time.<sup>7,8</sup> Traditionally, block copolymer self-assembly has been achieved via two steps: (i) initial molecular dissolution of the copolymer chains and (ii) reduction of the solvency for one of the blocks to drive microphase separation. For example, the Eisenberg group dissolved poly(4-vinylpyridine)–polystyrene (P4VP–PS) diblock copolymers in *N,N*-dimethylformamide (DMF) and gradually added either water or methanol (non-solvents for PS) to induce the formation of spherical micelles.<sup>9</sup> They later showed that more complex morphologies (e.g., spheres, rods, or vesicles) could be produced by the same approach using poly(acrylic acid)–PS (PAA–PS) diblock copolymers with varying degrees of polymerization (DPs) of the two blocks.<sup>10,11</sup> The development of living radical polymerization (LRP) chemistries<sup>12–15</sup> over the past two decades has enabled the synthesis of many new *functional* diblock copolymers. A wide range of diblock copolymer nano-objects has been prepared using post-polymerization processing routes, including cylindrical (or worm-like) micelles,<sup>16–18</sup> vesicles (or polymerosomes),<sup>19,20</sup> shell cross-linked micelles,<sup>21,22</sup> toroids,<sup>23</sup> schizophrenic micelles<sup>24,25</sup> and vesicles,<sup>26</sup> and micellar gels<sup>27–29</sup> as well as more complex morphologies.<sup>30–32</sup> However, final copolymer concentrations are rather low (<1.0% w/w) in almost all cases, which precludes many potential commercial applications.

Over the past eight years, considerable attention has been focused on developing an alternative route to produce block copolymer nano-objects known as polymerization-induced self-assembly (PISA). Typically, a soluble homopolymer (A) is chain-extended using a second monomer in a suitable solvent

such that the growing second block (B) gradually becomes insoluble, which drives *in situ* self-assembly to form AB diblock copolymer nano-objects. The A block is usually prepared via solution polymerization and acts as a steric stabilizer, while the insoluble B block is prepared via either dispersion or aqueous emulsion polymerization (depending on the monomer solubility in the continuous phase). This process is shown schematically in Scheme 1. By varying the DPs of the two blocks, either spheres or higher order morphologies (e.g., worms or vesicles) can be obtained. In principle, PISA syntheses can be conducted using any type of living polymerization,<sup>38–43</sup> but in practice, the majority of literature

**Scheme 1. Schematic of the Synthesis of Diblock Copolymer Nano-Objects via Polymerization-Induced Self-Assembly (PISA)**



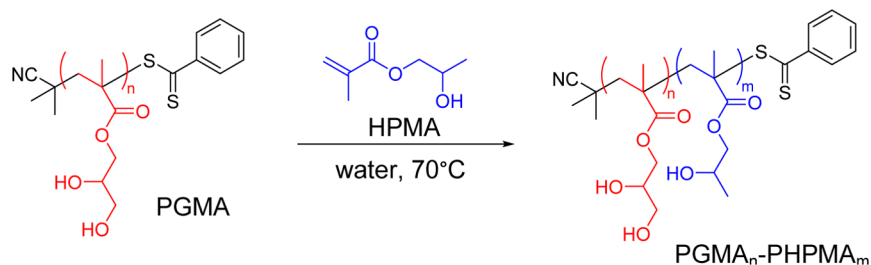
**Received:** December 1, 2015

**Revised:** February 1, 2016

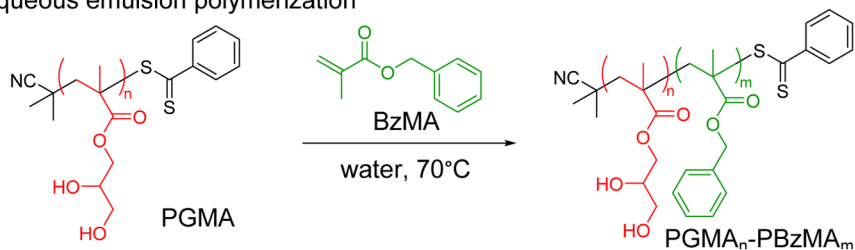
**Published:** March 9, 2016

Scheme 2. Examples of PISA Formulations Mediated by (a) RAFT Aqueous Dispersion Polymerization,<sup>33,34</sup> (b) RAFT Aqueous Emulsion Polymerization,<sup>35</sup> (c) RAFT Alcoholic Dispersion Polymerization,<sup>36</sup> and (d) RAFT Dispersion Polymerization in *n*-Alkanes<sup>37</sup>

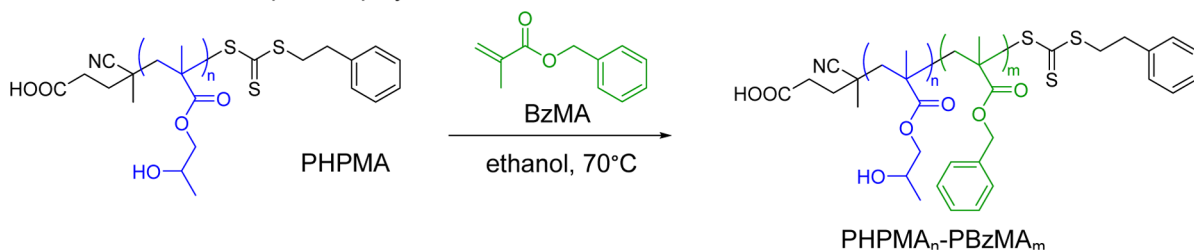
(a) RAFT aqueous dispersion polymerization



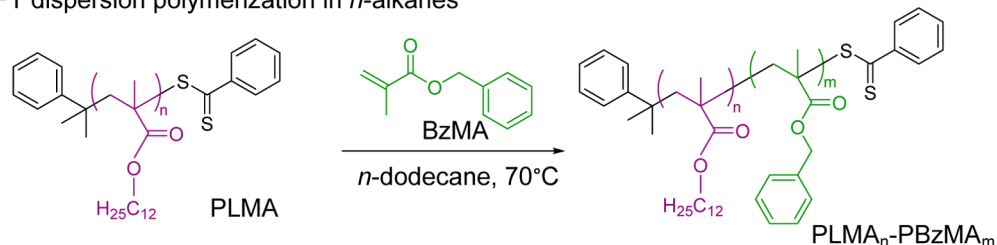
(b) RAFT aqueous emulsion polymerization



(c) RAFT alcoholic dispersion polymerization



(d) RAFT dispersion polymerization in *n*-alkanes



examples are based on reversible addition–fragmentation chain transfer (RAFT) polymerization.<sup>33,44–53</sup> This radical-based chemistry enables PISA syntheses to be conducted with many functional monomers in a wide range of solvents, including water,<sup>33,54,55</sup> polar solvents (such as lower alcohols),<sup>49,56–63</sup> non-polar solvents (such as *n*-alkanes, mineral oil, and poly( $\alpha$ -olefins)),<sup>37,49,64–67</sup> and also more exotic media such as ionic liquids.<sup>68</sup> One very important advantage of such PISA formulations is that reactions can be conducted at relatively high solids (25–50% w/w).<sup>54,56,57,64</sup> The versatility of this approach is illustrated in Scheme 2, which shows PISA formulations in water, ethanol, and *n*-dodecane. The same poly(glycerol monomethacrylate) (PGMA) stabilizer block can be used for either the RAFT aqueous dispersion polymerization of 2-hydroxypropyl methacrylate (HPMA)<sup>33,34,69,70</sup> or the RAFT aqueous emulsion polymerization of benzyl methacrylate (BzMA).<sup>35</sup> BzMA can also be used as the core-forming block for RAFT dispersion polymerization in polar solvents, such as ethanol, using a PHPMA stabilizer<sup>36</sup> or for RAFT dispersion

polymerization in non-polar solvents, such as *n*-heptane, *n*-dodecane, or mineral oil, using a poly(lauryl methacrylate) (PLMA) stabilizer.<sup>37,64,66</sup> These particular literature examples serve to demonstrate that just four blocks can provide the basis for four different PISA formulations.

In many cases the final copolymer morphology is dictated primarily by the relative volume fractions of the two blocks, as described by the packing parameter ( $P$ ).<sup>75,76</sup> In addition to spheres, worms, and vesicles,<sup>33,34,36,37,55,60,61,65,69,77–85</sup> other unusual morphologies have also been produced by PISA, such as lamellae,<sup>72</sup> framboidal vesicles,<sup>86</sup> spaced concentric vesicles,<sup>74</sup> and yolk/shell particles.<sup>62</sup> Examples of these morphologies are shown in Figure 1. Other examples of unusual morphologies produced by RAFT-mediated PISA include large compound vesicles<sup>60,77,78,87</sup> and doughnuts.<sup>88</sup> This wide range of well-defined morphologies illustrates the versatility and remarkable control afforded by PISA. However, the painstaking construction of phase diagrams is essential for the reproducible targeting of desired pure copolymer morpholo-

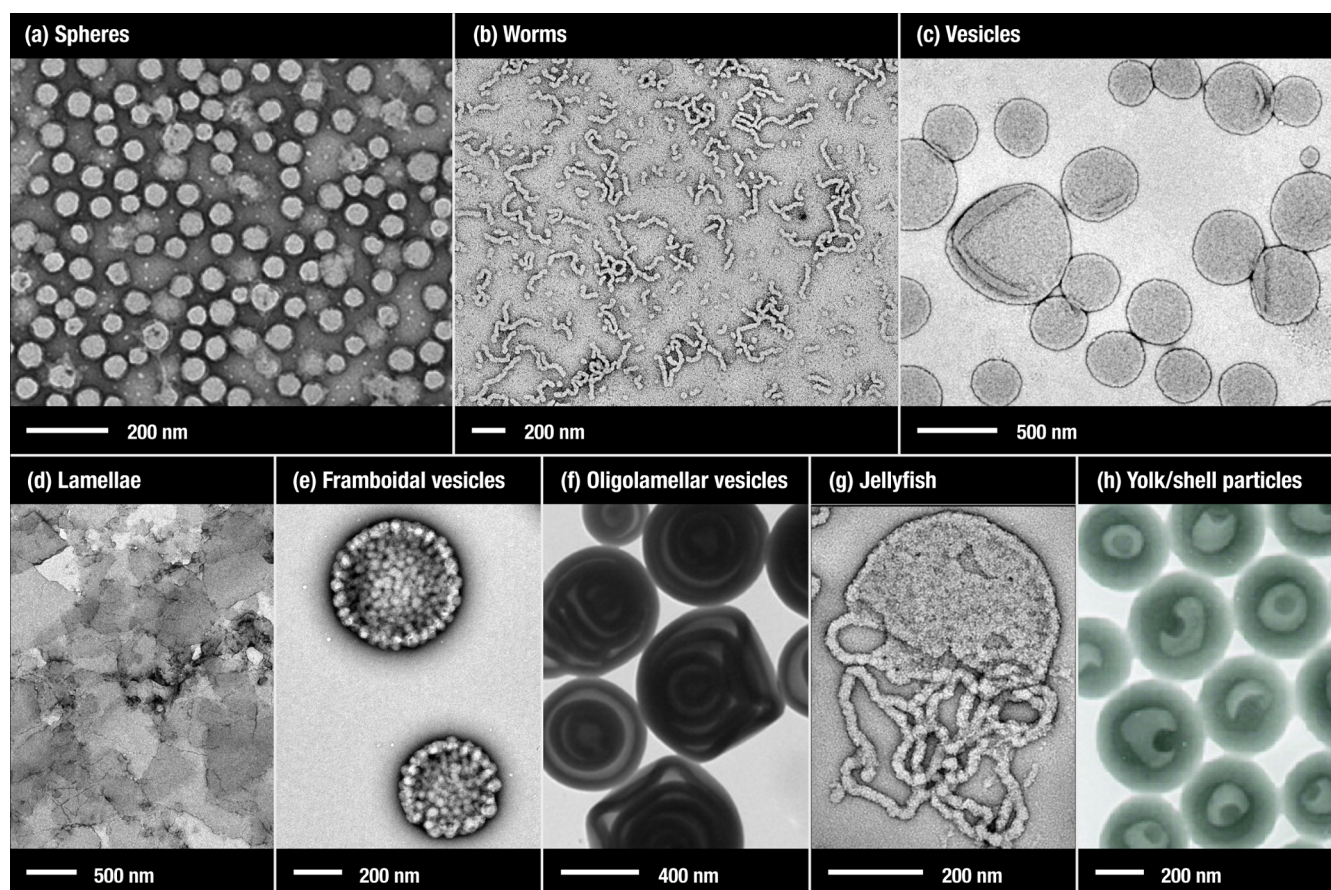


**Figure 1.** Representative transmission electron microscopy (TEM) images for various morphologies that can be synthesized using RAFT-mediated PISA. (a) Poly(quaternized 2-(dimethylamino) ethyl methacrylate)-*stat*-glycerol monomethacrylate)-poly(2-hydroxypropyl methacrylate) (P(QDMA<sub>11</sub>-*stat*-GMA<sub>116</sub>)-PHPMA<sub>900</sub>) spheres.<sup>71</sup> (b) Poly(glycerol monomethacrylate)-poly(2-hydroxypropyl methacrylate) (PGMA<sub>47</sub>-PHPMA<sub>130</sub>) worms.<sup>69</sup> (c) Poly(glycerol monomethacrylate)-poly(2-hydroxypropyl methacrylate) (PGMA<sub>47</sub>-PHPMA<sub>200</sub>) vesicles.<sup>69</sup> (d) Poly(methacrylic acid)-poly(styrene-*alt*-*N*-phenylmaleimide) (PMAA<sub>79</sub>-P(St-*alt*-NMI)<sub>650</sub>) lamellae.<sup>72</sup> (e) Poly(glycerol monomethacrylate)-poly(2-hydroxypropyl methacrylate)-poly(benzyl methacrylate) (PGMA<sub>63</sub>-PHPMA<sub>350</sub>-PBzMA<sub>125</sub>) framboidal vesicles.<sup>73</sup> (f) Poly(4-vinylpyridine)-polystyrene (P4VP<sub>73</sub>-PS<sub>654</sub>) oligolamellar vesicles.<sup>74</sup> (g) Poly(glycerol monomethacrylate)-poly(2-hydroxypropyl methacrylate) (PGMA<sub>47</sub>-PHPMA<sub>156</sub>, PGMA<sub>47</sub>-PHPMA<sub>200</sub> at 78% HPMA conversion) jellyfish.<sup>69</sup> (h) Poly(4-vinylpyridine)-polystyrene (P4VP-PS) and homopolystyrene yolk/shell nanoparticles.<sup>62</sup> (a) Reproduced with permission from ref 71. (b, c, g) Reproduced with permission from ref 69. (d) Reproduced with permission from ref 72. (e) Previously unpublished image. (f) Reproduced with permission from ref 74. (h) Reproduced with permission from ref 62.

gies.<sup>34,36,37,59,65,72,89</sup> This rational approach has enabled the synthesis of various types of well-defined spherical nanoparticles<sup>33,35</sup> and also low-polydispersity vesicles.<sup>90</sup> Block copolymer worms are invariably well-defined in terms of their mean widths but typically exhibit a relatively broad distribution of worm lengths. Nevertheless, PISA syntheses remain the best synthetic route to produce concentrated dispersions of block copolymer worms, which is highly desirable for studying their rheological behavior. In this Perspective, the various advantages offered by RAFT-mediated PISA formulations are discussed along with some of the current drawbacks and problems associated with this platform technology.

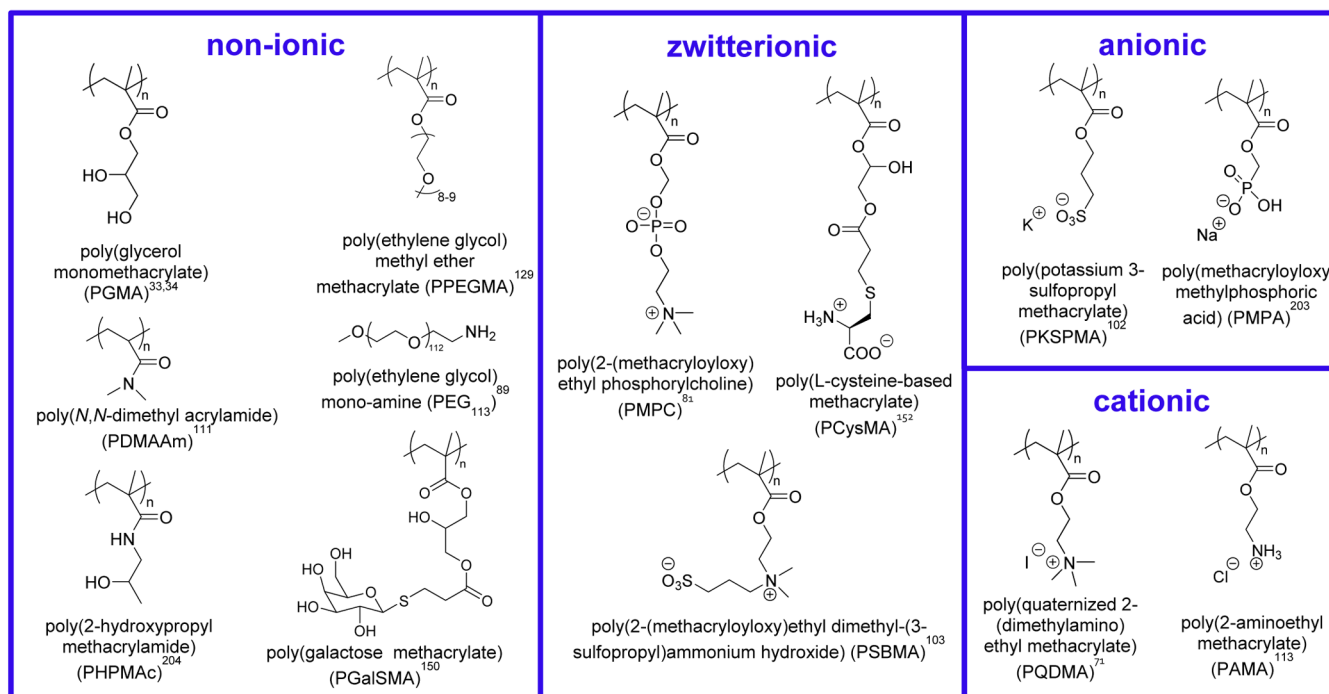
#### ■ COMPARISON OF AQUEOUS PISA FORMULATIONS WITH CONVENTIONAL AQUEOUS EMULSION POLYMERIZATION

Conventional aqueous emulsion polymerization involves free radical polymerization rather than RAFT polymerization; it is highly efficient and can be conveniently conducted at high solids.<sup>91</sup> Hence, it is worth asking whether RAFT-mediated PISA formulations offer any advantages over such a well-

established, commercially successful technology. If near-monodisperse spherical particles of 100–1000 nm diameter are desired, then conventional aqueous emulsion polymerization is clearly superior to aqueous RAFT-mediated PISA formulations. Both approaches enable high monomer conversions to be achieved within 1–2 h at 60–70 °C, but significantly narrower particle size distributions and a much wider range of mean particle diameters can be produced using conventional aqueous emulsion polymerization. However, if relatively small spheres of (say) 20–50 nm diameter are desired, then aqueous PISA offers a potentially decisive advantage because it does not require high levels of added surfactant. In this context, it is worth emphasizing that aqueous emulsion polymerization formulations often suffer from excess surfactant, which is known to compromise performance<sup>92</sup> and whose removal via either centrifugation or dialysis is not normally cost-effective. Moreover, if sterically stabilized particles are required, then an optimized aqueous PISA formulation usually offers high blocking efficiencies (and hence effective steric stabilization) via *surfactant-free* formulations.<sup>35,69,76,79,93–96</sup> This is in striking contrast to the relatively



## a) aqueous dispersion polymerization



## b) aqueous emulsion polymerization

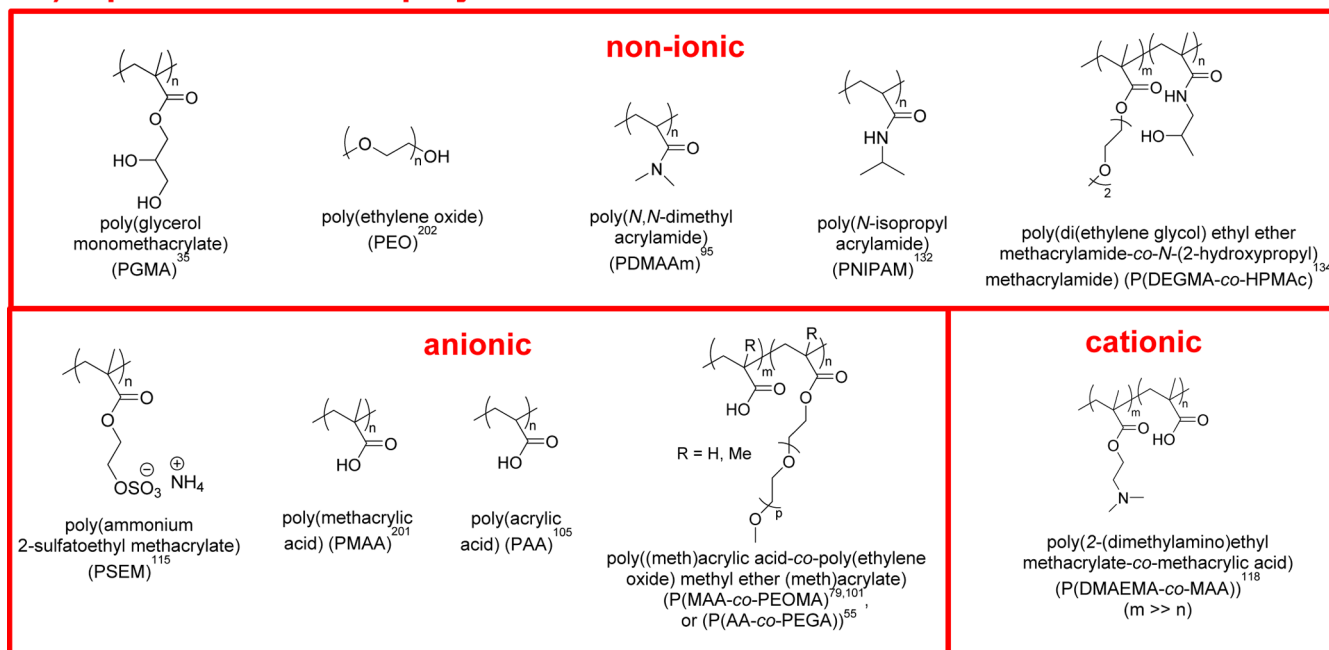


**Figure 2.** Chemical structures of various types of steric stabilizer blocks utilized for (a) RAFT-mediated aqueous dispersion polymerization and (b) RAFT-mediated aqueous emulsion polymerization.

low grafting efficiencies usually achieved when using either macromonomers, block copolymers, or graft copolymer stabilizers for aqueous emulsion polymerization.<sup>97–100</sup>

Possibly the most important advantage offered by RAFT aqueous emulsion polymerization over conventional aqueous emulsion polymerization is the ability to prepare diblock copolymer worms and vesicles. However, this has only been achieved for a small minority of PISA syntheses,<sup>55,79,80,101</sup> whereas many RAFT aqueous dispersion polymerization

formulations enable access to such “higher order” morphologies.<sup>34,46,54,70,71,89,102,103</sup> Most literature examples of RAFT aqueous emulsion polymerization syntheses only result in the formation of kinetically-trapped spheres, even when targeting highly asymmetric diblock compositions.<sup>35,95,96,104,105</sup> These observations are currently not properly understood and surely warrant further work. In contrast, most RAFT dispersion polymerization formulations typically exhibit the expected range of copolymer morphologies (spheres, worms, and



vesicles) provided that such syntheses are conducted at relatively high solids (>20% w/w) while using a sufficiently short stabilizer block as a macromolecular chain transfer agent (macro-CTA). The latter aspect is important because a relatively long stabilizer block leads to highly effective steric stabilization immediately after micellar nucleation. This prevents efficient sphere–sphere fusion, which is the essential first step in the production of anisotropic worms.<sup>54</sup>

It should be noted that targeting a spherical morphology via PISA can offer important advantages. First, the solution viscosity is dramatically reduced for spherical nanoparticles compared to the equivalent synthesis of molecularly-dissolved block copolymer chains via solution polymerization. Additionally, the onset of micellar nucleation during the production of spherical nanoparticles is typically followed by a significantly faster rate of polymerization.<sup>69,102,106,107</sup> This is because the unreacted monomer diffuses into the nascent nanoparticle cores in order to solvate the growing insoluble block. This leads to a higher local monomer concentration and enables aqueous PISA syntheses to be completed within 2 h at 70 °C. Similar, albeit less pronounced, rate enhancements are also observed for *n*-alkane PISA formulations.<sup>37</sup> However, alcoholic PISA syntheses appear to be significantly slower, often requiring 24 h for 95% conversion<sup>36,56,57</sup> and sometimes considerably longer.<sup>60</sup> Moreover, in at least some cases no rate enhancement is observed to achieve such formulations.<sup>72,108</sup> Currently, this striking difference is not understood. It is known that substantially faster polymerizations can be achieved for alcoholic RAFT PISA formulations simply by adding water as a co-solvent.<sup>61,106</sup> This is most likely because (i) water is a non-solvent for the growing core-forming PBzMA or polystyrene block, leading to particle nucleation at a shorter critical DP, and (ii) both BzMA and styrene each have relatively low solubility in water, so addition of water to the continuous phase should promote stronger monomer partitioning within the growing diblock copolymer nuclei. However, it is also well-known that the radical polymerization of various vinyl monomers is significantly faster in dilute aqueous solution compared to bulk polymerization.<sup>109,110</sup> This suggests that the water co-solvent could be playing an additional role at the molecular level in PISA syntheses conducted in alcohol/water mixtures.

## ■ SURFACE CHEMISTRY OF BLOCK COPOLYMER NANO-OBJECTS

In principle, the nature of the steric stabilizer block should dictate the surface chemistry of the resulting block copolymer nano-objects. For example, aqueous RAFT-mediated PISA can be conducted with a wide range of steric stabilizers under both dispersion (Figure 2a) and emulsion conditions (Figure 2b). This approach enables the design of a wide range of spheres, worms, or vesicles exhibiting nonionic,<sup>34,89,111</sup> zwitterionic,<sup>81,103,112</sup> anionic,<sup>102</sup> or cationic<sup>56,71,113</sup> character in the case of RAFT aqueous dispersion polymerization. Similarly, RAFT aqueous emulsion polymerization has been used to produce non-ionic,<sup>35,114</sup> anionic,<sup>105,115–117</sup> or cationic spheres.<sup>118</sup> As expected, the chemical nature of the stabilizer block directly influences the colloidal stability of the nanoparticles. Thus, choosing a zwitterionic polysulfobetaine (PSBMA) block confers enhanced salt tolerance,<sup>103</sup> a non-ionic poly(glycerol monomethacrylate) (PGMA) block enables pH-modulated selective adsorption of nanoparticles onto a micropatterned planar substrate,<sup>35</sup> and an anionic poly-

(ammonium 2-sulfatoethyl methacrylate) (PSEM) block promotes efficient occlusion within ZnO host crystals.<sup>115</sup>

Since the chemical nature of the stabilizer block determines the surface wettability of the particles (or particle contact angle<sup>119</sup>), *hydrophilic* diblock copolymer nanoparticles can be designed to stabilize oil-in-water Pickering emulsions.<sup>35,73,120</sup> Similarly, *hydrophobic* diblock copolymer nanoparticles can be designed to stabilize water-in-oil emulsions.<sup>121</sup> By judiciously combining these two types of nanoparticles (and optimizing the homogenization conditions), Thompson and co-workers exploited PISA to produce Pickering *double emulsions*.<sup>122</sup> In this case, both types of Pickering emulsifier possessed a worm-like morphology. Block copolymer worms were found to adsorb much more strongly at the oil–water interface than the more commonly employed spheres because the former nanoparticles exhibit a relatively high surface area per unit mass.<sup>120</sup> Similarly, Mable and co-workers recently reported that *framboidal* PGMA–PHPMA–PBzMA vesicles are much more efficiently adsorbed at the oil–water interface than the equivalent *smooth* PGMA–PHPMA vesicles.<sup>120</sup> This model system illustrates the importance of surface roughness on Pickering emulsifier performance.

## ■ STIMULUS-RESPONSIVE BLOCK COPOLYMER NANO-OBJECTS

There are various literature reports describing thermoresponsive block copolymer nano-objects prepared via PISA. Typically, these syntheses are based on RAFT aqueous dispersion polymerization rather than RAFT aqueous emulsion polymerization. Presumably, this is because the less hydrophobic core-forming block is more readily plasticized by water in the former case.<sup>35</sup> For PGMA–PHPMA block copolymer worms prepared in water, a worm-to-sphere transition can be induced simply by *cooling* from around 20–25 °C to 5–10 °C.<sup>123,124</sup> In contrast, for PLMA–PBzMA worms prepared via PISA in *n*-dodecane, Fielding et al. showed that *heating* up to 90 °C was required to induce the same order–order transition.<sup>66</sup> The temperature-dependent gel moduli for the two systems are shown in Figure 3. Similar worm-to-sphere transitions were subsequently reported by Pei et al. on heating various methacrylic diblock copolymer worms prepared in either *n*-tetradecane or ethanol.<sup>125,126</sup> In each case, the thermally-triggered transformation of highly anisotropic worms into isotropic spheres results in degelation. This is because the multiple inter-worm contacts in the initial gel are lost, which results in the formation of free-flowing dispersions.

According to Fielding et al., the switch in copolymer morphology is a direct result of *surface plasticization* of the core-forming block, which leads to a reduction in the effective packing parameter.<sup>66</sup> Reasonably good thermoreversibility can be observed, provided that the copolymer concentrations are in the 5–20% w/w range. However, on returning to the original temperature, the complementary sphere-to-worm transitions are not observed at lower copolymer concentrations (< 1% w/w), presumably because the one-dimensional (1D) fusion of multiple spheres is less probable under these conditions. The concentration dependence of the (ir)reversibility of such thermal transitions warrants further attention and is the subject of ongoing research in our laboratory.

Thermoresponsive core–shell nanoparticles have also been reported by An et al.<sup>127</sup> Chain extension of a poly(ethylene glycol) (PEG)-based macro-CTA with 2-methoxyethyl acrylate (MEA), PEG methyl ether acrylate, and a small amount of PEG

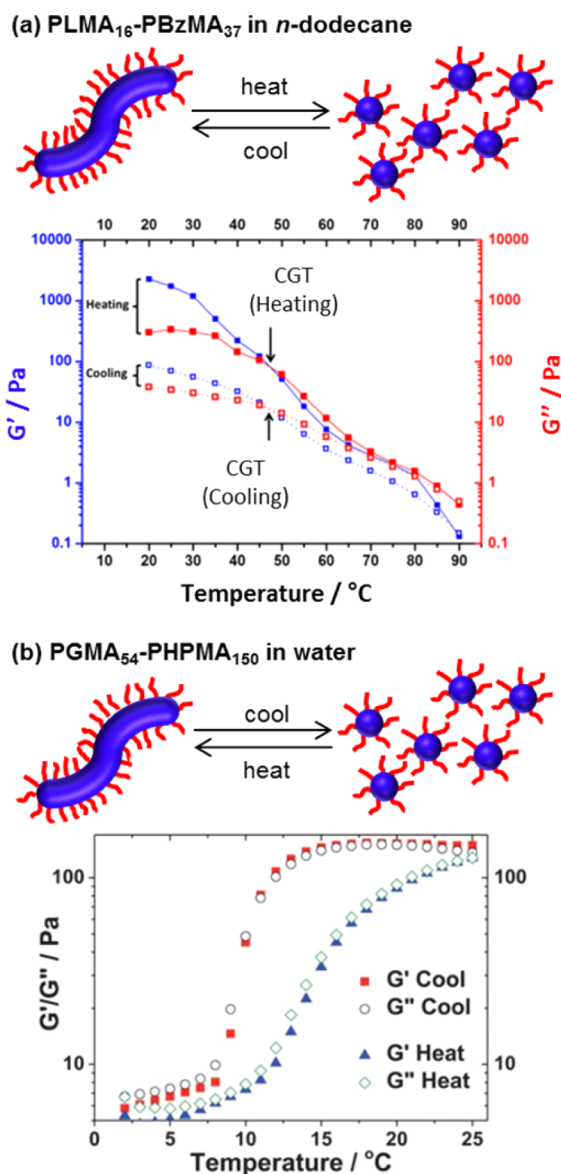


**Figure 3.** Temperature-dependent gel moduli as a result of worm-to-sphere transitions observed for (a) a PLMA<sub>16</sub>–PBzMA<sub>37</sub> worm gel in *n*-dodecane at 20% w/w solids<sup>66</sup> and (b) an aqueous PGMA<sub>54</sub>–PHPMA<sub>150</sub> worm gel at 10% w/w solids.<sup>124</sup> (a) Reproduced with permission from ref 66. (b) Reproduced with permission from ref 124. Copyright 2012 The Royal Society of Chemistry.

diacrylate (PEGDA) cross-linker produced spherical nanogels, whose dimensions decreased almost linearly as the solution temperature was increased from 20 to 60 °C.<sup>127</sup> Other examples of thermoresponsive nanogels from the same group include a PEG-based macro-CTA chain-extended with MEA and a small amount of PEGDA cross-linker, which formed well-defined spherical nanogels up to 32% solids<sup>128</sup> and core-shell nanogels composed of either linear or branched PEG-based shells and methacrylic cores.<sup>129</sup> Core dehydration was observed by <sup>1</sup>H NMR on heating above 40 °C. Spectroscopy studies indicated subtle differences in hydrogen bonding between the core-forming blocks and the surrounding water molecules.<sup>130</sup> Similar thermoresponsive nanogels were also prepared by Rieger et al.<sup>131</sup> In this case, PEG-based macro-CTAs were chain-extended with a mixture of *N,N'*-diethylacrylamide (DEAAm) and *N,N'*-methylene bis(acrylamide) via RAFT

aqueous dispersion copolymerization, with *in situ* cross-linking resulting in the formation of thermosensitive nanogels.

There are also recent reports of block copolymer worms prepared using a thermoresponsive stabilizer block. Monteiro and co-workers used a range of chain-end functional poly(*N*-isopropylacrylamide) (PNIPAM) macro-CTAs to polymerize styrene at 70 °C, well above the lower critical solution temperature (LCST) of PNIPAM, in a RAFT aqueous emulsion polymerization.<sup>132</sup> On cooling to 23 °C, below the LCST, worms were formed with multifunctional groups located at the surface, allowing further coupling reactions or chemical transformations to be made. It is, however, important to note that the addition of toluene was required to plasticize the PS cores. Moreover, strictly speaking this is not an example of a conventional PISA formulation as the PNIPAM block is above its LCST during the polymerization of styrene and hence not able to act as a steric stabilizer for the PS block. Instead, colloidal stability is maintained via addition of an anionic surfactant. These thermoresponsive worms were used in combination with PNIPAM functionalized with cell-binding vitronectin protein to bridge and aggregate human embryonic stem cells (hESCs), allowing 3D cell growth and exploiting the thermoresponsive properties to allow breakdown and subsequent reformation of the hESC aggregates.<sup>133</sup> Similarly, Davis et al. examined the RAFT aqueous emulsion polymerization of styrene but, in this case, used a poly(di(ethylene glycol) ethyl ether methacrylate-*co*-*N*-(2-hydroxypropyl)methacrylamide) (P(DEGMA-*co*-HPMAc)) stabilizer.<sup>134</sup> Cooling from 70 to 23 °C, below the cloud point temperature of the thermoresponsive stabilizing block, led to restructuring of the copolymer assemblies from spheres to worm-like nanoparticles or vesicles. However, this again required the addition of toluene to plasticize the PS cores.

pH-responsive diblock copolymer nano-objects have been prepared via PISA by Lovett et al.<sup>135</sup> and Penfold et al.<sup>136</sup> In the first case,<sup>135</sup> a carboxylic acid-functionalized RAFT CTA was used to prepare anionic PGMA–PHPMA worms via RAFT aqueous dispersion polymerization at around pH 3. Under these conditions, the terminal carboxylic acid group ( $pK_a \approx 4.7$ ) is in its protonated neutral form and a soft aqueous worm gel was obtained at 10% solids. Adjusting the solution pH to 6 led to ionization of the weakly acidic end-groups, thus increasing the relative volume fraction of the stabilizer block. This subtle change was sufficient to induce a worm-to-sphere transition, which caused *in situ* degelation. This order–order transition proved to be reversible: a worm gel was reformed on lowering the solution pH. Because there is only one ionizable acid group per copolymer chain, relatively little acid or base is required to induce the morphological transition compared to traditional pH-responsive block copolymers. However, this subtle pH-responsive behavior is suppressed in the presence of salt because of charge screening. The second example of pH-responsive diblock copolymer nano-objects prepared by PISA<sup>136</sup> is again based on PGMA–PHPMA worms, but in this case they possess tertiary amine end-groups arising from a morpholine-functionalized RAFT CTA. A worm gel prepared at pH 7–7.5 at 15% solids underwent a worm-to-sphere transition on acidification to pH 3, causing *in situ* degelation as the morpholine end-groups became protonated. This order–order transition is fully reversible in salt-free solutions, but in the presence of added electrolyte, the terminal cationic charge is screened, which enables the worm gels to remain intact. These complementary examples illustrate that the judicious

selection of an appropriate RAFT CTA can be used to confer pH-responsive behavior on ostensibly *non-ionic* diblock copolymers while requiring minimal amounts of added base or acid.

Another example of stimuli-responsive nano-objects prepared by PISA has been recently reported by Zetterlund et al.<sup>137</sup> In this case the stimulus is gaseous CO<sub>2</sub>, which enables the copolymer morphology to be fine-tuned. Alcoholic RAFT dispersion polymerization of styrene from a poly(4-vinylpyridine) (P4VP) macro-CTA was used to produce P4VP–PS diblock copolymer spheres, worms, or vesicles in the absence of CO<sub>2</sub> and spheres or worms in the presence of CO<sub>2</sub>. This weakly acidic gas interacted with the basic pyridine groups on the P4VP stabilizer block, which increased the relative volume of the block and hence lowered the effective packing parameter; thus, the introduction of CO<sub>2</sub> was used to make the formation of higher order morphologies less energetically favorable. Additionally, introduction of CO<sub>2</sub> led to (i) lower chain mobility in the core, (ii) reduced solvent polarity, leading to better solvation of the solvophobic block, hence shifting morphology transitions to higher DPs, and (iii) lower effective block copolymer concentrations, shifting the copolymer morphology toward spheres. Moreover, the phase space for pure worms, which is typically rather narrow and hence somewhat elusive,<sup>34</sup> proved to be much more readily accessible in the presence of CO<sub>2</sub>.

## CHARACTERIZATION TECHNIQUES

Much of the PISA literature has focused on core-forming blocks based on either methacrylic monomers or styrene. Such polymers have relatively high glass transition temperatures ( $T_g$ ),<sup>138</sup> which aids their characterization by transmission electron microscopy (TEM). In contrast, there are far fewer studies involving acrylic formulations. The low  $T_g$  of acrylic polymers compared to their methacrylic counterparts results in a strong tendency toward film formation during TEM grid preparation, producing images that are not representative of the true copolymer morphology in solution.<sup>139</sup> In this case rigorous morphological characterization requires cryo-TEM, which is a much more expensive, time-consuming, and less widely available technique. Nevertheless, it seems likely that all-acrylic PISA formulations will be explored in more detail in the near future, particularly if film-forming nano-objects offer a decisive advantage for commercial applications.

Another powerful characterization tool is small-angle X-ray scattering (SAXS). Unlike TEM, this technique enables systems to be characterized directly as dispersions. Moreover, statistically robust particle dimensions can be obtained since X-ray scattering is averaged over many millions of nano-objects. In contrast, TEM studies typically sample only a few hundred to a few thousand particles and are hence prone to sampling bias. Provided that a physically realistic model is employed, SAXS studies enable the dimensions of nano-objects to be calculated with precision. In contrast, techniques such as dynamic light scattering (DLS) merely report diffusion coefficients, which are indirectly related to the particle size via the Stokes–Einstein equation (which assumes a spherical morphology). Nevertheless, selection of an appropriate scattering model for SAXS analysis is usually informed by some prior knowledge regarding the particle size and morphology of the nano-objects. This is normally provided by imaging techniques, such as TEM. Static light scattering (SLS) has also been used to characterize diblock copolymer nano-objects prepared via PISA. This technique

reports the radius of gyration ( $R_g$ ) and the weight-average particle mass, with the latter parameter typically being used to calculate the particle aggregation number,  $N_{agg}$ .<sup>141–143</sup> In two recent studies  $N_{agg}$  data obtained via SLS has been compared to that calculated from SAXS analyses, with good agreement providing greater confidence in the model used for the latter technique.<sup>142,143</sup>

Mykhaylyk and co-workers have demonstrated that SAXS can be used to characterize spheres, worms, and vesicles prepared via PISA.<sup>65,66,73,90,121,123,144,145</sup> For example, SAXS analysis of vesicles formed during the RAFT aqueous dispersion polymerization of HPMA (Figure 4) has revealed an

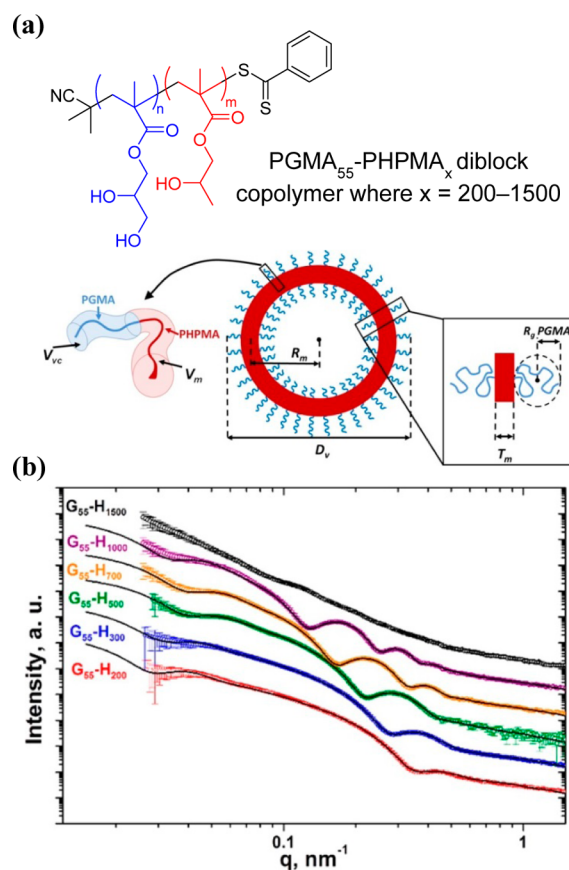


**Figure 4.** Chemical structure and schematic representation (a) and experimental SAXS patterns (b) of PGMA<sub>55</sub>–PHPMA<sub>x</sub> diblock copolymer vesicles (where  $x = 200, 300, 500, 700, 1000,$  or  $1500$ ) prepared via RAFT aqueous dispersion polymerization. All but one of the SAXS curves could be well-fitted using a vesicle model, which reveals an approximately constant outer vesicle diameter  $D_v$  as the vesicle membrane  $T_m$  thickens with increasing  $x$ . The exception is PGMA<sub>55</sub>–PGMA<sub>1500</sub>, which has a nonvesicular morphology as judged by TEM studies. Reproduced with permission from ref 140.

unexpected growth mechanism for this morphology. As the DP of the core-forming PHPMA block increases, the vesicle membrane thickens, but the outer vesicle diameter is conserved, which leads to a gradual reduction in the vesicle lumen volume.<sup>140</sup> Geometric considerations confirm that this is actually the *only* mechanism by which the growing vesicles can minimize their total interfacial area and hence their free energy. Moreover, this mechanism places an important constraint on vesicle growth. As longer core-forming blocks are targeted, the vesicle morphology eventually becomes



unstable as a result of increasing steric congestion of stabilizer chains within the inner leaflet combined with greater solvent plasticization of the vesicle membrane. It is rather difficult to imagine any other *single* characterization technique providing such detailed mechanistic insights.

## POTENTIAL APPLICATIONS AND OPPORTUNITIES FOR PISA FORMULATIONS

There have been various reports of highly efficient “one-pot” PISA syntheses based on RAFT aqueous emulsion polymerization,<sup>101,104,105,107,116</sup> RAFT aqueous dispersion polymerization,<sup>70</sup> and RAFT *n*-alkane dispersion polymerization.<sup>64</sup> Such advances seem to be particularly promising for potential commercial applications, which have begun to emerge as this subdiscipline has matured. In this context, there has been significant recent progress in the efficient removal of RAFT end-groups from copolymer chains using various reagents,<sup>146–149</sup> although it remains to be seen whether such strategies are equally effective for copolymer *nanoparticles* (as opposed to soluble chains). While such post-polymerization modification undoubtedly adds both cost and complexity to PISA syntheses, this approach may yet be cost-effective for certain high-value biomedical applications suggested for block copolymer nanoparticles.<sup>123,133,150–152</sup> Nevertheless, the relatively high cost, intrinsic color, and malodorous nature of the sulfur-based RAFT CTAs may well prove to be detrimental to the development of next-generation paints and coatings or even relatively “high-value” cosmetics additives. On the other hand, it is perhaps worth emphasizing that a series of RAFT-synthesized star copolymers have already been commercialized by the Lubrizol Corporation as high-performance thickeners for automotive engine oils.<sup>153,154</sup> Thus, RAFT chemistry is commercially viable for at least some industrial sectors.

RAFT polymerization is not a prerequisite for PISA syntheses, which have also been conducted using nitroxide-mediated polymerization (NMP)<sup>38–40</sup> and atom transfer radical polymerization (ATRP).<sup>41–43</sup> However, although the downsides of RAFT chemistry are thereby avoided, such formulations often suffer from either incomplete conversions (NMP) or metal catalyst contamination (ATRP). One recent synthetic development is single electron transfer living radical polymerization (SET-LRP).<sup>155</sup> SET-LRP proceeds under mild reaction conditions in various solvents<sup>156–160</sup> and can be used for a wide range of monomers.<sup>156,157,161–166</sup> Very recently, SET-LRP has been utilized by Cunningham and co-workers for growing either one or two poly(methyl methacrylate) (PMMA) chains from an alginate-based macroinitiator in methanol/water mixtures to produce alginate-stabilized PMMA-core spheres.<sup>167</sup> PISA syntheses using organotellurium-mediated living radical polymerization (TERP)<sup>168,169</sup> have also been attempted.<sup>170</sup> For example, *tert*-butyl acrylate and styrene were polymerized using a PMAA-based macroTERP agent producing triblock copolymer nanoparticles,<sup>171</sup> although significant improvements in control over  $M_w/M_n$  and/or blocking efficiency seem to be desirable to warrant wider use of this chemistry.

In 2011, Blanz et al.<sup>69</sup> monitored the RAFT aqueous dispersion polymerization of HPMA using TEM for a formulation targeting vesicles as the final copolymer morphology. More specifically, an evolution in copolymer morphology from spheres to worms to vesicles was observed, with jellyfish being identified as a key intermediate structure between the latter two nano-objects. Given the “open” structure of such jellyfish (see Figure 1), one interesting question that certainly

warrants exploration is whether encapsulation can be achieved *in situ* when targeting vesicles as the final copolymer morphology. In this context, it is worth emphasizing that small molecules are likely to permeate through such vesicle membranes rather quickly, but soluble macromolecules or nanoparticles should be retained much more efficiently. Indeed, significant progress toward this goal has just been reported by Zhang, Sumerlin, and co-workers.<sup>172</sup> Photoinitiated RAFT polymerization of HPMA was conducted using a PEG macro-CTA in the presence of an aqueous silica sol, with TEM studies providing reasonable evidence for nanoparticle encapsulation within the resulting PEG–PHPMA vesicles. Moreover, a model globular protein (bovine serum albumin, BSA) could also be incorporated within the same vesicles, although no direct visual evidence for this encapsulated species was possible. Unusually, these PISA syntheses were conducted at 25 °C, which makes *in situ* protein denaturation highly unlikely. In closely related work, we have shown that the aqueous RAFT dispersion polymerization of HPMA using a PGMA macro-CTA in the presence of silica nanoparticles enabled their *in situ* encapsulation inside the resulting PGMA–PHPMA vesicles, as confirmed by TEM and SAXS studies (Figure 5).<sup>173</sup> This

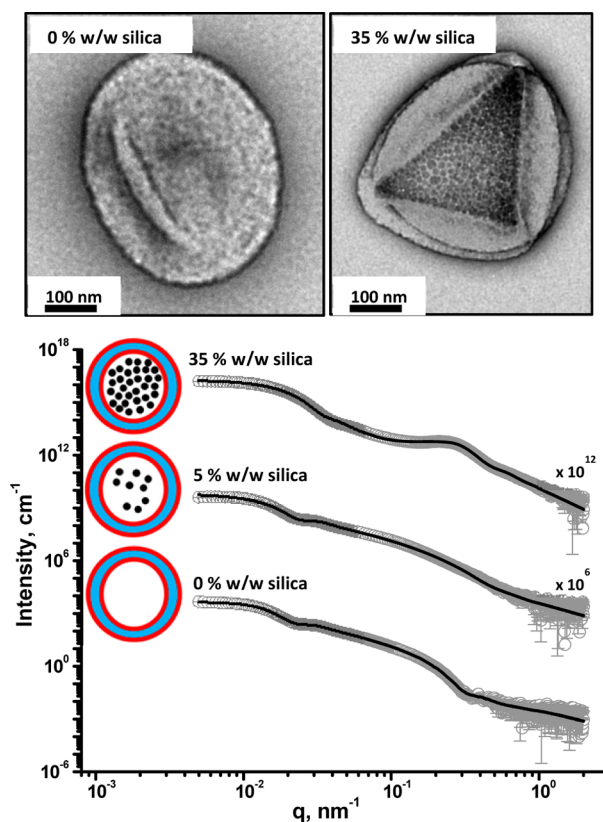


**Figure 5.** TEM images (top) and SAXS patterns (bottom) obtained for PGMA<sub>58</sub>–PHPMA<sub>250</sub> diblock copolymer vesicles synthesized by RAFT aqueous dispersion polymerization in the presence of increasing amounts of silica nanoparticles (0, 5, and 35% w/w silica) after six centrifugation–redispersion cycles to remove excess silica. For the SAXS data, gray circles represent experimental data and solid lines represent fitting curves. For clarity, the upper two SAXS patterns are shifted vertically by arbitrary scaling factors, as shown on the plot. Inset: schematic representation of empty and silica-loaded PGMA<sub>58</sub>–PHPMA<sub>250</sub> diblock copolymer vesicles, where small black circles represent silica nanoparticles, red = PGMA block, and light blue = PHPMA block.

was followed by thermally-triggered release of the silica payload on cooling to 0–10 °C, since this induces a vesicle-to-sphere transition. Furthermore, BSA could be encapsulated intact by conducting the polymerization at 37 °C using a low-temperature initiator, thus avoiding its denaturation. The BSA loading efficiency was determined to be 11% by fluorescence spectroscopy, although TEM suggested protein flocculation.

In the absence of any attractive interactions between the block copolymer chains and the encapsulated species, the theoretical *maximum* encapsulation efficiency is simply given by the ratio of the total vesicle lumen volume to the total solution volume; this suggests that the majority of the silica nanoparticles or protein molecules cannot be encapsulated within the vesicles. Nevertheless, if these two studies can be extended to include enzymes or antibodies, then this *in situ* encapsulation approach suggests potential biomedical applications, especially if triggered release could be achieved under biologically relevant conditions.<sup>174,175</sup> In related work, Davis et al. reported that Nile Red could be encapsulated within poly(oligoethylene glycol methacrylate)–polystyrene (POEGMA–PS) vesicles during the one-pot RAFT alcoholic dispersion polymerization of styrene.<sup>176</sup> However, the final monomer conversions were relatively low (10%). Moreover, the amount of encapsulated dye was stated to be more than the original dye concentration. This suggests that light scattering from the vesicles artificially increased the apparent absorbance of the dye, which would invalidate the encapsulation assay.

It is well-known that the target DP for a RAFT polymerization is equal to the monomer concentration divided by the macro-CTA concentration.<sup>44</sup> Given that the upper limit of concentration for PISA syntheses is of the order of 50% solids,<sup>35,64</sup> lowering the macro-CTA concentration under such conditions becomes the only available means of increasing the target DP of the core-forming block. However, the initiator concentration must be reduced accordingly, because RAFT polymerizations are typically conducted at [macro-CTA]/[initiator] molar ratios of 3 to 10<sup>35,62</sup> so as to minimize the proportion of dead chains while maintaining an acceptable polymerization rate.<sup>52,177</sup> Thus, targeting very high DPs eventually leads to either gradual loss of RAFT control or no polymerization at all (because there is insufficient initiator to generate the required radical flux). Clearly, the precise upper limit DP will vary significantly depending on (i) the monomer class (e.g., methacrylate vs acrylate vs styrene), (ii) initiator type (due to the differing characteristic half-lives at a given temperature), (iii) nature of the CTA (dithiobenzoate vs trithiocarbonate vs xanthate), and (iv) the precise PISA formulation (e.g., RAFT aqueous emulsion polymerization vs RAFT aqueous dispersion polymerization).

Nevertheless, RAFT-mediated PISA formulations possess some intrinsic advantages over RAFT solution polymerization. It is well-recognized that PISA syntheses can be very efficient, with very high monomer conversions often being achieved within short reaction times.<sup>34,69,89,107,131,150,178–181</sup> The marked rate acceleration that typically occurs during PISA syntheses, as discussed previously, usually coincides with the onset of micellar nucleation and, as noted by Blanazs et al.,<sup>69</sup> can lead to a five-fold increase in the rate of polymerization. In addition, copolymer chains are produced in the form of low-viscosity nanoparticle dispersions rather than high-viscosity solutions. Hence it seems likely that RAFT-mediated PISA should enable higher DPs to be targeted for the core-forming block within reasonable time scales. There are already several examples of

PISA formulations with relatively high DP core-forming blocks. For example, we have previously reported DPs of up to 1000 for the RAFT aqueous dispersion polymerization of HPMA.<sup>65</sup> In as-yet unpublished work, we have recently achieved DPs of up to 4700 when utilizing a highly polar methacrylic monomer. Similarly, Davis et al. recently reported polystyrene-core block copolymer spheres with molecular weights above 10<sup>6</sup> g mol<sup>-1</sup> (corresponding to polystyrene DPs around 14 000) via RAFT aqueous emulsion polymerization at 80 °C.<sup>96</sup> High conversions (>90%) were attained in 6 h with polydispersities remaining at 1.40 or below.

Blanazs et al. reported that PGMA–PHPMA worms prepared via RAFT aqueous dispersion polymerization of HPMA can form soft, free-standing biocompatible hydrogels.<sup>123,124</sup> Gelation is believed to be the result of multiple inter-worm contacts, rather than worm entanglements. Moreover, these worm gels proved to be thermoresponsive: cooling from 20–25 °C to around 5–10 °C induced a reversible worm-to-sphere transition, which led to *in situ* degelation (Figure 4b). Unlike other PHPMA-based diblock copolymers,<sup>89,103</sup> this morphological switch is fully reversible and provides a convenient route to sterilization via cold ultrafiltration. Very recently, such worm gels have been examined as 3D matrices for human stem cell colonies, with protein assays indicating that the stem cells enter stasis (G<sub>0</sub> state) within 16 h of immersion within the worm gel. Such quiescent cells can survive for up to 2 weeks at 37 °C without passaging. On cooling to 5–10 °C, degelation occurs, and the stem cell colonies can be readily removed from the copolymer aqueous dispersion. On returning to 37 °C, the stem cells slowly emerge from stasis over a 16–24 h period while retaining their original pluripotent character. Thus, these worm gels may offer a cost-effective alternative to cryo-preservation for global stem cell transportation.<sup>182</sup> Additionally, next-generation *thiol-functional* PGMA–PHPMA worm gels have been recently reported by Warren and co-workers.<sup>183</sup> These are currently being evaluated as potential muco-adhesive gels, while the gel reinforcement conferred by inter-worm disulfide cross-links<sup>184</sup> has just been demonstrated to be critical in the context of thermoreversible 3D hydrogels for “cells-in-gels-in-paper” applications.<sup>185</sup> Such wholly synthetic worm gels offer an interesting alternative to animal-derived products such as *Matrigel*.

## ■ LIMITATIONS OF PISA FORMULATIONS

Armes and co-workers demonstrated that when targeting *linear* diblock copolymer chains, the worm and vesicle morphologies that can be accessed via PISA cannot tolerate the presence of surfactant.<sup>86,120</sup> In particular, addition of *ionic* surfactants to colloiddally stable aqueous vesicular dispersions led to rapid dissociation, producing either spheres or molecularly dissolved copolymer chains.<sup>186</sup> In principle, this problem can be overcome by cross-linking the copolymer chains, either during their PISA synthesis by addition of a bifunctional monomer such as ethylene glycol dimethacrylate<sup>120,86,187</sup> or by post-polymerization derivatization.<sup>186</sup> This typically requires the cross-linker to be added as a third block rather than via statistical copolymerization. This is because the latter approach tends to result in a loss of colloidal stability. The former cross-linking protocol works well for spheres<sup>112,188</sup> and vesicles<sup>189,186</sup> and can also work for worms,<sup>120,187</sup> although it is somewhat less reliable for this morphology. Unfortunately, such covalent cross-linking also eliminates the desirable stimulus-responsive behavior, which most likely precludes certain potential

applications for worms (as smart thickeners) and vesicles (for encapsulation/release applications) in home and personal care applications.

Another obvious limitation of the PISA approach is for monomers that are non-solvents for the corresponding core-forming block. For example, in our early exploratory PISA syntheses we attempted to prepare diblock copolymer nanoparticles consisting of a core-forming polyacrylonitrile block in water. Acrylonitrile monomer has appreciable aqueous solubility, and its polymerization initially proceeded smoothly in homogeneous solution. However, once the critical DP for nucleation was attained (as judged by the appearance of Tyndall scattering<sup>190</sup>), essentially no further polymerization occurred because the remaining unreacted monomer does not solvate the polyacrylonitrile cores. In principle, this problem could be addressed by adding a suitable co-solvent. However, this would necessarily produce a non-aqueous formulation, which would negate the various advantages conferred by using water as a polymerization medium. Fortunately, there are very few vinyl monomers that are not good solvents for their corresponding homopolymer, so this problem is rather rare in practice.

It is well-documented that reproducible PISA syntheses require the construction of detailed phase diagrams.<sup>34,56,59,64–66,70,72,89,90,103,150,152,155,172,191</sup> This is particularly true if the worm phase is desired, since this morphology typically occupies rather narrow phase space. This is usually the case regardless of the PISA formulation, with strikingly similar core-forming block DP vs copolymer concentration phase diagrams being observed for RAFT dispersion polymerizations conducted in water, alcohols, or *n*-alkanes.<sup>34,37,56</sup> Typical phase diagrams for PGMA<sub>78</sub>–PHPMA<sub>*x*</sub> and PGMA<sub>47</sub>–PHPMA<sub>*x*</sub> syntheses via RAFT aqueous dispersion polymerization of HPMA are shown in Figure 6.<sup>54</sup> In each case, a large batch of macro-CTA is first prepared, since it is difficult to reproducibly target precise stabilizer DPs at the intermediate conversions required to ensure chain-end fidelity. Hence a single large batch of macro-CTA is used to carry out a series of subsequent multiple small-scale PISA syntheses. For most methacrylic or styrene-based PISA formulations, assignment of the final copolymer morphology at approximately full monomer conversion can be made via conventional TEM studies. Generally speaking, it is good practice to examine a partially constructed phase diagram in order to inform further PISA syntheses, with the aim being to minimize uncertainty in the positions of the various phase boundaries.<sup>103</sup>

Unlike traditional block copolymer phase diagrams depicting equilibrium morphologies, the lower concentration regions of PISA phase diagrams often correspond to kinetically trapped morphologies (typically spheres). This is certainly the case for the PGMA<sub>78</sub>–PHPMA<sub>*x*</sub> phase diagram shown in Figure 6a. In contrast, the PGMA<sub>47</sub>–PHPMA<sub>*x*</sub> phase diagram shown in Figure 6b has little or no concentration dependence. Presumably, this is because this shorter PGMA block is a less effective steric stabilizer, which makes the multiple 1D fusion of spheres much more likely to occur on the time scale of the PISA synthesis. This is the critical event that enables access to higher order morphologies, in addition to the spheres initially formed during nucleation.

Currently, there are no PISA syntheses that provide good control over the mean worm length. This appears to be a formidable technical challenge, but recent success in the rational design of low-polydispersity vesicles<sup>90</sup> suggests that

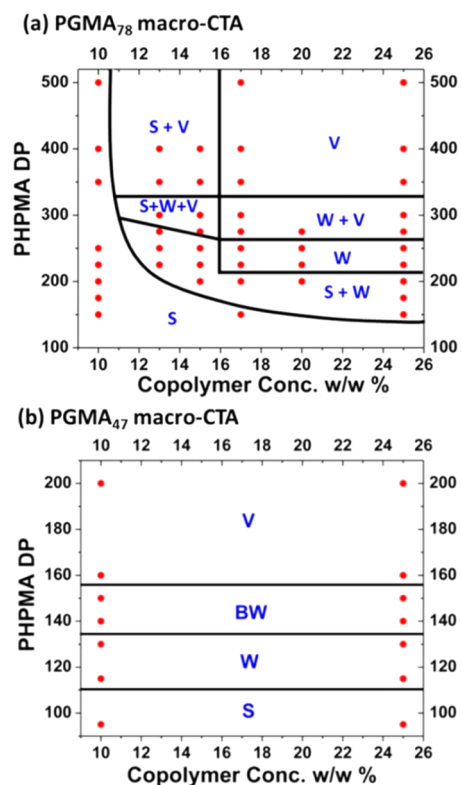


**Figure 6.** Phase diagrams reported for a series of (a) PGMA<sub>78</sub>–PHPMA<sub>*x*</sub> and (b) PGMA<sub>47</sub>–PHPMA<sub>*x*</sub> copolymer nano-objects synthesized by aqueous RAFT dispersion polymerization of HPMA for copolymer concentrations ranging from 10% to 25% w/w. S = spherical micelles, W = worms, BW = branched worms, and V = vesicles. Adapted with permission from ref 34.

there may be some scope in this regard. One possibility may be to take advantage of a thermoreversible sphere-to-worm transition and introduce an “initiator” type nanoparticle to ensure that the 1D fusion of multiple spheres occurs from a predefined number of nucleation sites. A similar concept has been recently reported by the Manners group for the construction of well-defined cylinders based on the principle of crystallization-driven self-assembly.<sup>192</sup> Alternatively, Monteiro and co-workers have recently described an interesting strategy for generating tadpole-like morphologies via a so-called “temperature-directed morphological transformation”. In principle, this approach may also have some merit for the production of low-polydispersity worms.<sup>193</sup>

Another important constraint lies in our current inability to use the packing parameter *P* in order to predict final copolymer morphologies for PISA formulations. This is not particularly surprising because this simple geometric concept simply cannot accommodate the relative degrees of solvation (and hence effective volume fractions) of the stabilizer and core-forming blocks. This problem is further exacerbated because *P* is also likely to be sensitive to an unknown degree of monomer solvation of the core-forming block once nucleation has occurred. Moreover, the packing parameter concept cannot account for the known concentration dependence of certain PISA syntheses.<sup>34</sup> Furthermore, we are currently unable to explain, even qualitatively, why many (but not all) RAFT aqueous emulsion polymerization formulations lead solely to kinetically-trapped spheres.<sup>35,96</sup> Unfortunately, even for favorable situations where equilibrium copolymer morphologies are



produced, it is not yet possible to predict the positions of phase boundaries for PISA syntheses.<sup>194</sup> Clearly, theoretical advances would be particularly welcome for enhancing our understanding of these fascinating and versatile formulations.

## SUMMARY AND PROSPECT

For the synthesis of a wide range of block copolymer nano-objects, PISA formulations offer decisive advantages in terms of versatility, efficiency, and cost-effectiveness. This generic approach is beginning to transform the subdiscipline of “polymer colloids” while also offering a remarkably diverse range of potential commercial applications. However, in several important aspects, our fundamental understanding of various PISA formulations remains frustratingly incomplete. Nevertheless, there are now numerous literature examples whereby PISA has provided a highly convenient route to new types of block copolymer nanoparticles. This has enabled fundamental scientific advances to be made in the design of bespoke Pickering emulsifiers,<sup>121,122,195</sup> nanosized vehicles for intracellular delivery of fluorescent probes,<sup>150</sup> rational design of transparent dispersions,<sup>196</sup> stimulus-responsive gels,<sup>66,124,135,136</sup> nanoparticle-loaded vesicles prepared directly at high solids,<sup>172,173</sup> model organic nanoparticles for occlusion within inorganic host crystals,<sup>115</sup> nanoparticle lubricants for engine oils,<sup>64,197</sup> nanoparticles for catalysis applications,<sup>188,198</sup> efficient encapsulation of pigment particles,<sup>199</sup> and sterilizable 3D hydrogels for various biomedical applications, including the preservation of human stem cells and red blood cells.<sup>123,182,200</sup>

In summary, PISA is now widely recognized as an important platform technology for the design of bespoke nano-objects of controllable size, shape, and surface chemistry. This fast-maturing subdiscipline is expected to become an important component in the toolbox of the synthetic polymer chemist.

## AUTHOR INFORMATION

### Corresponding Author

\*E-mail [s.p.armes@shef.ac.uk](mailto:s.p.armes@shef.ac.uk) (S.P.A.).

### Notes

The authors declare no competing financial interest.

### Biographies



Sarah L. Canning studied chemistry at the University of Sheffield (UK) and the University at Buffalo, SUNY (USA). She completed a CASE PhD at the University of Sheffield in 2015 under the supervision of Professors Stephen Rimmer and Mark Geoghegan, sponsored by Domino UK Ltd. She is now working in the research group of Professor Steven Armes. Her current research interests include the synthesis, characterization, and self-assembly of amphiphilic copoly-

mers using controlled radical polymerization techniques and polymerization-induced self-assembly, with a particular focus on the aqueous RAFT emulsion polymerization of less-activated monomers.



Gregory N. Smith studied chemistry at the University of Bristol (UK) and graduated with a MSci in 2007. He continued at the same institution and was awarded a PhD under the supervision of Professor Julian Eastoe in 2015. He is currently working as a research associate in synthetic polymer chemistry at the University of Sheffield (UK) investigating polymerization-induced self-assembly. His research interests concern the self-assembly and surface interactions of soft matter from small molecules to macromolecules. He has a particular interest in colloids in non-polar media, electrokinetics, and applications of small-angle scattering.



Prof. Steven P. Armes graduated from the University of Bristol (BSc 1983 and PhD 1987). After a two-year postdoc stint at Los Alamos National Laboratory in New Mexico, he accepted a lectureship at Sussex University. He was promoted to Professor in 2000 and moved to the University of Sheffield in 2004. He has published more than 540 papers (H-index = 94), received the Tilden medal from the Royal Society of Chemistry in 2013, and was elected as a fellow of the Royal Society in 2014. His current research activities are focused on polymerization-induced self-assembly (PISA).

## ACKNOWLEDGMENTS

S.P.A. thanks the ERC for a five-year Advanced Investigator grant (PISA 320372) and the EPSRC for a Platform grant (EP/J007846/1).

## REFERENCES

(1) Nagarajan, R. One Hundred Years of Micelles: Evolution of the Theory of Micellization. In *Surfactant Science and Technology, Retrospects and Prospects*; CRC Press: 2014.

- (2) McBain, J. W. Mobility of Highly-Charged Micelles. *Trans. Faraday Soc.* **1913**, *9*, 99–101.
- (3) Climie, I. E.; White, E. F. T. The Aggregation of Random and Block Copolymers Containing Acrylonitrile in Mixed Solvents. *J. Polym. Sci.* **1960**, *47*, 149–156.
- (4) Burnett, G. M.; Meares, P.; Paton, C. Styrene + Methyl Methacrylate Block Copolymers. Part 2.-Behaviour in Dilute Solutions. *Trans. Faraday Soc.* **1962**, *58*, 737–746.
- (5) Newman, S. Note on Colloidal Dispersions from Block Copolymers. *J. Appl. Polym. Sci.* **1962**, *6*, S15–S16.
- (6) Krause, S. Dilute Solution Properties of a Styrene–Methyl Methacrylate Block Copolymer. *J. Phys. Chem.* **1964**, *68*, 1948–1955.
- (7) Szwarc, M.; Levy, M.; Milkovich, R. Polymerization Initiated By Electron Transfer to Monomer. A New Method of Formation of Block Polymers. *J. Am. Chem. Soc.* **1956**, *78*, 2656–2657.
- (8) Szwarc, M. “Living” Polymers. *Nature* **1956**, *178*, 1168–1169.
- (9) Gao, Z.; Varshney, S. K.; Wong, S.; Eisenberg, A. Block Copolymer “Crew-Cut” Micelles in Water. *Macromolecules* **1994**, *27*, 7923–7927.
- (10) Zhang, L.; Eisenberg, A. Multiple Morphologies of “Crew-Cut” Aggregates of Polystyrene-*b*-Poly(acrylic acid) Block Copolymers. *Science* **1995**, *268*, 1728–1731.
- (11) Zhang, L.; Eisenberg, A. Multiple Morphologies and Characteristics of “Crew-Cut” Micelle-like Aggregates of Polystyrene-*b*-Poly(acrylic acid) Diblock Copolymers in Aqueous Solutions. *J. Am. Chem. Soc.* **1996**, *118*, 3168–3181.
- (12) Patten, T. E.; Matyjaszewski, K. Atom Transfer Radical Polymerization and the Synthesis of Polymeric Materials. *Adv. Mater.* **1998**, *10*, 901–915.
- (13) Hawker, C. J.; Bosman, A. W.; Harth, E. New Polymer Synthesis by Nitroxide Mediated Living Radical Polymerizations. *Chem. Rev.* **2001**, *101*, 3661–3688.
- (14) Moad, G.; Rizzardo, E.; Thang, S. H. Living Radical Polymerization by the RAFT Process. *Aust. J. Chem.* **2005**, *58*, 379–410.
- (15) Braunecker, W. A.; Matyjaszewski, K. Controlled/living Radical Polymerization: Features, Developments, and Perspectives. *Prog. Polym. Sci.* **2007**, *32*, 93–146.
- (16) Won, Y.-Y.; Davis, H. T.; Bates, F. S. Giant Wormlike Rubber Micelles. *Science* **1999**, *283*, 960–963.
- (17) Dalhaimer, P.; Engler, A. J.; Parthasarathy, R.; Discher, D. E. Targeted Worm Micelles. *Biomacromolecules* **2004**, *5*, 1714–1719.
- (18) Geng, Y.; Discher, D. E. Hydrolytic Degradation of Poly(ethylene oxide)-*block*-Polycaprolactone Worm Micelles. *J. Am. Chem. Soc.* **2005**, *127*, 12780–12781.
- (19) Discher, B. M.; Won, Y.-Y.; Ege, D. S.; Lee, J. C.-M.; Bates, F. S.; Discher, D. E.; Hammer, D. A. Polymersomes: Tough Vesicles Made from Diblock Copolymers. *Science* **1999**, *284*, 1143–1146.
- (20) Discher, D. E.; Eisenberg, A. Polymer Vesicles. *Science* **2002**, *297*, 967–973.
- (21) Thurmond, K. B., II; Kowalewski, T.; Wooley, K. L. Water-Soluble Knedel-like Structures: The Preparation of Shell-Cross-Linked Small Particles. *J. Am. Chem. Soc.* **1996**, *118*, 7239–7240.
- (22) Read, E. S.; Armes, S. P. Recent Advances in Shell Cross-Linked Micelles. *Chem. Commun.* **2007**, *29*, 3021–3035.
- (23) Pochan, D. J.; Chen, Z.; Cui, H.; Hales, K.; Qi, K.; Wooley, K. L. Toroidal Triblock Copolymer Assemblies. *Science* **2004**, *306*, 94–97.
- (24) Bütün, V.; Liu, S.; Weaver, J. V. M.; Bories-Azeau, X.; Cai, Y.; Armes, S. P. A Brief Review of “Schizophrenic” Block Copolymers. *React. Funct. Polym.* **2006**, *66*, 157–165.
- (25) Arotçaréna, M.; Heise, B.; Ishaya, S.; Laschewsky, A. Switching the Inside and the Outside of Aggregates of Water-Soluble Block Copolymers with Double Thermoresponsivity. *J. Am. Chem. Soc.* **2002**, *124*, 3787–3793.
- (26) Rodríguez-Hernández, J.; Lecommandoux, S. Reversible Inside–Out Micellization of pH-Responsive and Water-Soluble Vesicles Based on Polypeptide Diblock Copolymers. *J. Am. Chem. Soc.* **2005**, *127*, 2026–2027.
- (27) Alexandridis, P.; Hatton, T. A. Poly(ethylene oxide)–Poly(propylene oxide)–Poly(ethylene oxide) Block Copolymer Surfactants in Aqueous Solutions and at Interfaces: Thermodynamics, Structure, Dynamics, and Modeling. *Colloids Surf. A* **1995**, *96*, 1–46.
- (28) Madsen, J.; Armes, S. P. (Meth)acrylic Stimulus-Responsive Block Copolymer Hydrogels. *Soft Matter* **2012**, *8*, 592–605.
- (29) Zhou, C.; Hillmyer, M. A.; Lodge, T. P. Efficient Formation of Multicompartment Hydrogels by Stepwise Self-Assembly of Thermoresponsive ABC Triblock Terpolymers. *J. Am. Chem. Soc.* **2012**, *134*, 10365–10368.
- (30) Wang, X.; Guerin, G.; Wang, H.; Wang, Y.; Manners, I.; Winnik, M. A. Cylindrical Block Copolymer Micelles and Co-Micelles of Controlled Length and Architecture. *Science* **2007**, *317*, 644–647.
- (31) Erhardt, R.; Zhang, M.; Böker, A.; Zettl, H.; Abetz, C.; Frederik, P.; Krausch, G.; Abetz, V.; Müller, A. H. E. Amphiphilic Janus Micelles with Polystyrene and Poly(methacrylic acid) Hemispheres. *J. Am. Chem. Soc.* **2003**, *125*, 3260–3267.
- (32) Christian, D. A.; Tian, A.; Ellenbroek, W. G.; Levental, I.; Rajagopal, K.; Janmey, P. A.; Liu, A. J.; Baumgart, T.; Discher, D. E. Spotted Vesicles, Striped Micelles and Janus Assemblies Induced by Ligand Binding. *Nat. Mater.* **2009**, *8*, 843–849.
- (33) Li, Y.; Armes, S. P. RAFT Synthesis of Sterically Stabilized Methacrylic Nanolatexes and Vesicles by Aqueous Dispersion Polymerization. *Angew. Chem., Int. Ed.* **2010**, *49*, 4042–4046.
- (34) Blanazs, A.; Ryan, A. J.; Armes, S. P. Predictive Phase Diagrams for RAFT Aqueous Dispersion Polymerization: Effect of Block Copolymer Composition, Molecular Weight, and Copolymer Concentration. *Macromolecules* **2012**, *45*, 5099–5107.
- (35) Cunningham, V. J.; Alswieleh, A. M.; Thompson, K. L.; Williams, M.; Leggett, G. J.; Armes, S. P.; Musa, O. M. Poly(glycerol monomethacrylate)–poly(benzyl methacrylate) Diblock Copolymer Nanoparticles via RAFT Emulsion Polymerization: Synthesis, Characterization, and Interfacial Activity. *Macromolecules* **2014**, *47*, 5613–5623.
- (36) Zehm, D.; Ratcliffe, L. P. D.; Armes, S. P. Synthesis of Diblock Copolymer Nanoparticles via RAFT Alcoholic Dispersion Polymerization: Effect of Block Copolymer Composition, Molecular Weight, Copolymer Concentration, and Solvent Type on the Final Particle Morphology. *Macromolecules* **2013**, *46*, 128–139.
- (37) Fielding, L. A.; Derry, M. J.; Ladmiral, V.; Rosselgong, J.; Rodrigues, A. M.; Ratcliffe, L. P. D.; Sugihara, S.; Armes, S. P. RAFT Dispersion Polymerization in Non-Polar Solvents: Facile Production of Block Copolymer Spheres, Worms and Vesicles in *n*-Alkanes. *Chem. Sci.* **2013**, *4*, 2081–2087.
- (38) Delaittre, G.; Nicolas, J.; Lefay, C.; Save, M.; Charleux, B. Surfactant-Free Synthesis of Amphiphilic Diblock Copolymer Nanoparticles via Nitroxide-Mediated Emulsion Polymerization. *Chem. Commun.* **2005**, *1*, 614–616.
- (39) Brusseau, S.; D’Agosto, F.; Magnet, S.; Couvreur, L.; Chamignon, C.; Charleux, B. Nitroxide-Mediated Copolymerization of Methacrylic Acid and Sodium 4-Styrenesulfonate in Water Solution and One-Pot Synthesis of Amphiphilic Block Copolymer Nanoparticles. *Macromolecules* **2011**, *44*, 5590–5598.
- (40) Groison, E.; Brusseau, S.; D’Agosto, F.; Magnet, S.; Inoubli, R.; Couvreur, L.; Charleux, B. Well-Defined Amphiphilic Block Copolymer Nanoobjects via Nitroxide-Mediated Emulsion Polymerization. *ACS Macro Lett.* **2012**, *1*, 47–51.
- (41) Kim, K. H.; Kim, J.; Jo, W. H. Preparation of Hydrogel Nanoparticles by Atom Transfer Radical Polymerization of *N*-Isopropylacrylamide in Aqueous Media Using PEG Macro-Initiator. *Polymer* **2005**, *46*, 2836–2840.
- (42) Sugihara, S.; Sugihara, K.; Armes, S. P.; Ahmad, H.; Lewis, A. L. Synthesis of Biomimetic Poly(2-(methacryloyloxy)ethyl Phosphorylcholine) Nanolatexes via Atom Transfer Radical Dispersion Polymerization in Alcohol/Water Mixtures. *Macromolecules* **2010**, *43*, 6321–6329.
- (43) Sugihara, S.; Armes, S. P.; Lewis, A. L. One-Pot Synthesis of Biomimetic Shell Cross-Linked Micelles and Nanocages by ATRP in Alcohol/Water Mixtures. *Angew. Chem., Int. Ed.* **2010**, *49*, 3500–3503.



- (44) Chiefari, J.; Chong, Y. K. B.; Ercole, F.; Krstina, J.; Jeffery, J.; Le, T. P. T.; Mayadunne, R. T. A.; Meijs, G. F.; Moad, C. L.; Moad, G.; et al. Living Free-Radical Polymerization by Reversible Addition–Fragmentation Chain Transfer: The RAFT Process. *Macromolecules* **1998**, *31*, 5559–5562.
- (45) Moad, G.; Rizzardo, E.; Thang, S. H. Living Radical Polymerization by the RAFT Process—A First Update. *Aust. J. Chem.* **2006**, *59*, 669–692.
- (46) Rieger, J. Guidelines for the Synthesis of Block Copolymer Particles of Various Morphologies by RAFT Dispersion Polymerization. *Macromol. Rapid Commun.* **2015**, *36*, 1458–1471.
- (47) Charleux, B.; Delaittre, G.; Rieger, J.; D'Agosto, F. Polymerization-Induced Self-Assembly: From Soluble Macromolecules to Block Copolymer Nano-Objects in One Step. *Macromolecules* **2012**, *45*, 6753–6765.
- (48) Sun, J.-T.; Hong, C.-Y.; Pan, C.-Y. Formation of the Block Copolymer Aggregates via Polymerization-Induced Self-Assembly and Reorganization. *Soft Matter* **2012**, *8*, 7753–7767.
- (49) Derry, M. J.; Fielding, L. A.; Armes, S. P. Polymerization-Induced Self-Assembly of Block Copolymer Nanoparticles via RAFT Non-Aqueous Dispersion Polymerization. *Prog. Polym. Sci.* **2016**, *52*, 1–18.
- (50) Chong, Y. K.; Le, T. P. T.; Moad, G.; Rizzardo, E.; Thang, S. H. A More Versatile Route to Block Copolymers and Other Polymers of Complex Architecture by Living Radical Polymerization: The RAFT Process. *Macromolecules* **1999**, *32*, 2071–2074.
- (51) Moad, G.; Chiefari, J.; Chong, Y. K.; Krstina, J.; Mayadunne, R. T. A.; Postma, A.; Rizzardo, E.; Thang, S. H. Living Free Radical Polymerization with Reversible Addition–Fragmentation Chain Transfer (the Life of RAFT). *Polym. Int.* **2000**, *49*, 993–1001.
- (52) Hill, M. R.; Carmean, R. N.; Sumerlin, B. S. Expanding the Scope of RAFT Polymerization: Recent Advances and New Horizons. *Macromolecules* **2015**, *48*, 5459–5469.
- (53) Sun, J.-T.; Hong, C.-Y.; Pan, C.-Y. Recent Advances in RAFT Dispersion Polymerization for Preparation of Block Copolymer Aggregates. *Polym. Chem.* **2013**, *4*, 873–881.
- (54) Warren, N. J.; Armes, S. P. Polymerization-Induced Self-Assembly of Block Copolymer Nano-Objects via RAFT Aqueous Dispersion Polymerization. *J. Am. Chem. Soc.* **2014**, *136*, 10174–10185.
- (55) Boissé, S.; Rieger, J.; Belal, K.; Di-Cicco, A.; Beaunier, P.; Li, M.-H.; Charleux, B. Amphiphilic Block Copolymer Nano-Fibers via RAFT-Mediated Polymerization in Aqueous Dispersed System. *Chem. Commun.* **2010**, *46*, 1950–1952.
- (56) Semsarilar, M.; Jones, E. R.; Blanazs, A.; Armes, S. P. Efficient Synthesis of Sterically-Stabilized Nano-Objects via RAFT Dispersion Polymerization of Benzyl Methacrylate in Alcoholic Media. *Adv. Mater.* **2012**, *24*, 3378–3382.
- (57) Jones, E. R.; Semsarilar, M.; Blanazs, A.; Armes, S. P. Efficient Synthesis of Amine-Functional Diblock Copolymer Nanoparticles via RAFT Dispersion Polymerization of Benzyl Methacrylate in Alcoholic Media. *Macromolecules* **2012**, *45*, 5091–5098.
- (58) Semsarilar, M.; Ladmiral, V.; Blanazs, A.; Armes, S. P. Poly(methacrylic acid)-Based AB and ABC Block Copolymer Nano-Objects Prepared via RAFT Alcoholic Dispersion Polymerization. *Polym. Chem.* **2014**, *5*, 3466–3475.
- (59) Semsarilar, M.; Penfold, N. J. W.; Jones, E. R.; Armes, S. P. Semi-Crystalline Diblock Copolymer Nano-Objects Prepared via RAFT Alcoholic Dispersion Polymerization of Stearyl Methacrylate. *Polym. Chem.* **2015**, *6*, 1751–1757.
- (60) Zhao, W.; Gody, G.; Dong, S.; Zetterlund, P. B.; Perrier, S. Optimization of the RAFT Polymerization Conditions for the *in situ* Formation of Nano-Objects via Dispersion Polymerization in Alcoholic Medium. *Polym. Chem.* **2014**, *5*, 6990–7003.
- (61) Zhang, X.; Rieger, J.; Charleux, B. Effect of the Solvent Composition on the Morphology of Nano-Objects Synthesized via RAFT Polymerization of Benzyl Methacrylate in Dispersed Systems. *Polym. Chem.* **2012**, *3*, 1502–1509.
- (62) Wan, W. M.; Pan, C. Y. Formation of Polymeric Yolk/Shell Nanomaterial by Polymerization-Induced Self-Assembly and Reorganization. *Macromolecules* **2010**, *43*, 2672–2675.
- (63) Wan, W. M.; Sun, X. L.; Pan, C. Y. Formation of Vesicular Morphologies via Polymerization Induced Self-Assembly and Reorganization. *Macromol. Rapid Commun.* **2010**, *31*, 399–404.
- (64) Derry, M. J.; Fielding, L. A.; Armes, S. P. Industrially-Relevant Polymerization-Induced Self-Assembly Formulations in Non-Polar Solvents: RAFT Dispersion Polymerization of Benzyl Methacrylate. *Polym. Chem.* **2015**, *6*, 3054–3062.
- (65) Lopez-Oliva, A. P.; Warren, N. J.; Rajkumar, A.; Mykhaylyk, O. O.; Derry, M. J.; Doncom, K. E. B.; Rymaruk, M. J.; Armes, S. P. Polydimethylsiloxane-Based Diblock Copolymer Nano-Objects Prepared in Nonpolar Media via RAFT-Mediated Polymerization-Induced Self-Assembly. *Macromolecules* **2015**, *48*, 3547–3555.
- (66) Fielding, L. A.; Lane, J. A.; Derry, M. J.; Mykhaylyk, O. O.; Armes, S. P. Thermo-Responsive Diblock Copolymer Worm Gels in Non-Polar Solvents. *J. Am. Chem. Soc.* **2014**, *136*, 5790–5798.
- (67) Houillot, L.; Bui, C.; Save, M.; Charleux, B.; Farcet, C.; Moire, C.; Raust, J.-A.; Rodriguez, I. Synthesis of Well-Defined Polyacrylate Particle Dispersions in Organic Medium Using Simultaneous RAFT Polymerization and Self-Assembly of Block Copolymers. A Strong Influence of the Selected Thiocarbonylthio Chain Transfer Agent. *Macromolecules* **2007**, *40*, 6500–6509.
- (68) Zhang, Q.; Zhu, S. Ionic Liquids: Versatile Media for Preparation of Vesicles from Polymerization-Induced Self-Assembly. *ACS Macro Lett.* **2015**, *4*, 755–758.
- (69) Blanazs, A.; Madsen, J.; Battaglia, G.; Ryan, A. J.; Armes, S. P. Mechanistic Insights for Block Copolymer Morphologies: How Do Worms Form Vesicles? *J. Am. Chem. Soc.* **2011**, *133*, 16581–16587.
- (70) Ratcliffe, L. P. D.; Ryan, A. J.; Armes, S. P. From a Water-Immiscible Monomer to Block Copolymer Nano-Objects via a One-Pot RAFT Aqueous Dispersion Polymerization Formulation. *Macromolecules* **2013**, *46*, 769–777.
- (71) Semsarilar, M.; Ladmiral, V.; Blanazs, A.; Armes, S. P. Cationic Polyelectrolyte-Stabilized Nanoparticles via RAFT Aqueous Dispersion Polymerization. *Langmuir* **2013**, *29*, 7416–7424.
- (72) Yang, P.; Ratcliffe, L. P. D.; Armes, S. P. Efficient Synthesis of Poly(methacrylic acid)-*block*-poly(styrene-*alt*-*N*-phenylmaleimide) Diblock Copolymer Lamellae Using RAFT Dispersion Polymerization. *Macromolecules* **2013**, *46*, 8545–8556.
- (73) Mable, C. J.; Warren, N. J.; Thompson, K. L.; Mykhaylyk, O. O.; Armes, S. P. Framboidal ABC Triblock Copolymer Vesicles: A New Class of Efficient Pickering Emulsifier. *Chem. Sci.* **2015**, *6*, 6179–6188.
- (74) Zhang, W.-J.; Hong, C.-Y.; Pan, C.-Y. Fabrication of Spaced Concentric Vesicles and Polymerizations in RAFT Dispersion Polymerization. *Macromolecules* **2014**, *47*, 1664–1671.
- (75) Israelachvili, J. N.; Mitchell, D. J.; Ninham, B. W. Theory of Self-Assembly of Hydrocarbon Amphiphiles into Micelles and Bilayers. *J. Chem. Soc., Faraday Trans. 2* **1976**, *72*, 1525–1568.
- (76) Blanazs, A.; Armes, S. P.; Ryan, A. J. Self-Assembled Block Copolymer Aggregates: From Micelles to Vesicles and Their Biological Applications. *Macromol. Rapid Commun.* **2009**, *30*, 267–277.
- (77) He, W. D.; Sun, X. L.; Wan, W. M.; Pan, C. Y. Multiple Morphologies of PAA-*b*-PSt Assemblies throughout RAFT Dispersion Polymerization of Styrene with PAA Macro-CTA. *Macromolecules* **2011**, *44*, 3358–3365.
- (78) Cai, W.; Wan, W.; Hong, C.; Huang, C.; Pan, C. Morphology Transitions in RAFT Polymerization. *Soft Matter* **2010**, *6*, 5554–5561.
- (79) Zhang, X.; Boissé, S.; Zhang, W.; Beaunier, P.; D'Agosto, F.; Rieger, J.; Charleux, B. Well-Defined Amphiphilic Block Copolymers and Nano-Objects Formed *in Situ* via RAFT-Mediated Aqueous Emulsion Polymerization. *Macromolecules* **2011**, *44*, 4149–4158.
- (80) Zhang, W.; D'Agosto, F.; Boyron, O.; Rieger, J.; Charleux, B. Toward a Better Understanding of the Parameters That Lead to the Formation of Nonspherical Polystyrene Particles via RAFT-Mediated One-Pot Aqueous Emulsion Polymerization. *Macromolecules* **2012**, *45*, 4075–4084.



- (81) Sugihara, S.; Blanazs, A.; Armes, S. P.; Ryan, A. J.; Lewis, A. L. Aqueous Dispersion Polymerization: A New Paradigm for in Situ Block Copolymer Self-Assembly in Concentrated Solution. *J. Am. Chem. Soc.* **2011**, *133*, 15707–15713.
- (82) Boissé, S.; Rieger, J.; Pembouong, G.; Beaunier, P.; Charleux, B. Influence of the Stirring Speed and CaCl<sub>2</sub> Concentration on the Nano-Object Morphologies Obtained via RAFT-Mediated Aqueous Emulsion Polymerization in the Presence of a Water-Soluble macroRAFT Agent. *J. Polym. Sci., Part A: Polym. Chem.* **2011**, *49*, 3346–3354.
- (83) Huang, C.-Q.; Pan, C.-Y. Direct Preparation of Vesicles from One-Pot RAFT Dispersion Polymerization. *Polymer* **2010**, *51*, 5115–5121.
- (84) Wan, W.-M.; Sun, X.-L.; Pan, C.-Y. Morphology Transition in RAFT Polymerization for Formation of Vesicular Morphologies in One Pot. *Macromolecules* **2009**, *42*, 4950–4952.
- (85) Wan, W.-M.; Hong, C.-Y.; Pan, C.-Y. One-Pot Synthesis of Nanomaterials via RAFT Polymerization Induced Self-Assembly and Morphology Transition. *Chem. Commun.* **2009**, *39*, 5883–5885.
- (86) Chambon, P.; Blanazs, A.; Battaglia, G.; Armes, S. P. Facile Synthesis of Methacrylic ABC Triblock Copolymer Vesicles by RAFT Aqueous Dispersion Polymerization. *Macromolecules* **2012**, *45*, 5081–5090.
- (87) Dan, M.; Huo, F.; Zhang, X.; Wang, X.; Zhang, W. Dispersion RAFT Polymerization of 4-Vinylpyridine in Toluene Mediated with the Macro-RAFT Agent of Polystyrene Dithiobenzoate: Effect of the Macro-RAFT Agent Chain Length and Growth of the Block Copolymer Nano-Objects. *J. Polym. Sci., Part A: Polym. Chem.* **2013**, *51*, 1573–1584.
- (88) Wan, W.-M.; Pan, C.-Y. One-Pot Synthesis of Polymeric Nanomaterials via RAFT Dispersion Polymerization Induced Self-Assembly and Re-Organization. *Polym. Chem.* **2010**, *1*, 1475–1484.
- (89) Warren, N. J.; Mykhaylyk, O. O.; Mahmood, D.; Ryan, A. J.; Armes, S. P. RAFT Aqueous Dispersion Polymerization Yields Poly(ethylene glycol)-Based Diblock Copolymer Nano-Objects with Predictable Single Phase Morphologies. *J. Am. Chem. Soc.* **2014**, *136*, 1023–1033.
- (90) Gonzato, C.; Semsarilar, M.; Jones, E. R.; Li, F.; Krooshof, G. J. P.; Wyman, P.; Mykhaylyk, O. O.; Tuinier, R.; Armes, S. P. Rational Synthesis of Low-Polydispersity Block Copolymer Vesicles in Concentrated Solution via Polymerization-Induced Self-Assembly. *J. Am. Chem. Soc.* **2014**, *136*, 11100–11106.
- (91) Lovell, P. A.; El-Aasser, M. S. *Emulsion Polymerization and Emulsion Polymers*; Wiley: 1997.
- (92) Guyot, A. Polymerizable Surfactants. *Curr. Opin. Colloid Interface Sci.* **1996**, *1*, 580–586.
- (93) Ferguson, C. J.; Hughes, R. J.; Nguyen, D.; Pham, B. T. T.; Gilbert, R. G.; Serelis, A. K.; Such, C. H.; Hawke, B. S. Ab Initio Emulsion Polymerization by RAFT-Controlled Self-Assembly. *Macromolecules* **2005**, *38*, 2191–2204.
- (94) Ferguson, C. J.; Hughes, R. J.; Pham, B. T. T.; Hawke, B. S.; Gilbert, R. G.; Serelis, A. K.; Such, C. H. Effective Ab Initio Emulsion Polymerization under RAFT Control. *Macromolecules* **2002**, *35*, 9243–9245.
- (95) Rieger, J.; Zhang, W.; Stoffelbach, F.; Charleux, B. Surfactant-Free RAFT Emulsion Polymerization Using Poly(*N,N*-dimethylacrylamide) Trithiocarbonate Macromolecular Chain Transfer Agents. *Macromolecules* **2010**, *43*, 6302–6310.
- (96) Truong, N. P.; Dussert, M. V.; Whittaker, M. R.; Quinn, J. F.; Davis, T. P. Rapid Synthesis of Ultrahigh Molecular Weight and Low Polydispersity Polystyrene Diblock Copolymers by RAFT-Mediated Emulsion Polymerization. *Polym. Chem.* **2015**, *6*, 3865–3874.
- (97) Charleux, B.; D'Agosto, F.; Delaittre, G. Preparation of Hybrid Latex Particles and Core-Shell Particles Through the Use of Controlled Radical Polymerization Techniques in Aqueous Media. *Adv. Polym. Sci.* **2010**, *233*, 125–183.
- (98) Bathfield, M.; D'Agosto, F.; Spitz, R.; Charreyre, M. T.; Pichot, C.; Delair, T. Sub-Micrometer Sized Hairy Latex Particles Synthesized by Dispersion Polymerization Using Hydrophilic Macromolecular RAFT Agents. *Macromol. Rapid Commun.* **2007**, *28*, 1540–1545.
- (99) Baines, F. L.; Dionisio, S.; Billingham, N. C.; Armes, S. P. Use of Block Copolymer Stabilizers for the Dispersion Polymerization of Styrene in Alcoholic Media. *Macromolecules* **1996**, *29*, 3096–3102.
- (100) Nzudie, D. T.; Dimonie, V. L.; Sudol, E. D.; El-Aasser, M. S. Use of Styrene-Maleic Anhydride Copolymers (SMA Resins) in Emulsion Copolymerization. *J. Appl. Polym. Sci.* **1998**, *70*, 2729–2747.
- (101) Zhang, W.; D'Agosto, F.; Dugas, P. Y.; Rieger, J.; Charleux, B. RAFT-Mediated One-Pot Aqueous Emulsion Polymerization of Methyl Methacrylate in Presence of Poly(methacrylic acid-co-poly(ethylene oxide) methacrylate) Trithiocarbonate Macromolecular Chain Transfer Agent. *Polymer* **2013**, *54*, 2011–2019.
- (102) Semsarilar, M.; Ladmiraal, V.; Blanazs, A.; Armes, S. P. Anionic Polyelectrolyte-Stabilized Nanoparticles via RAFT Aqueous Dispersion Polymerization. *Langmuir* **2012**, *28*, 914–922.
- (103) Doncom, K. E. B.; Warren, N. J.; Armes, S. P. Polysulfobetaine-Based Diblock Copolymer Nano-Objects via Polymerization-Induced Self-Assembly. *Polym. Chem.* **2015**, *6*, 7264–7273.
- (104) Zhang, W.; D'Agosto, F.; Boyron, O.; Rieger, J.; Charleux, B. One-Pot Synthesis of Poly(methacrylic acid-co-poly(ethylene oxide) methyl ether methacrylate)-*b*-polystyrene Amphiphilic Block Copolymers and Their Self-Assemblies in Water via RAFT-Mediated Radical Emulsion Polymerization. A Kinetic Study. *Macromolecules* **2011**, *44*, 7584–7593.
- (105) Chaduc, I.; Boyron, O.; Charleux, B.; D'Agosto, F.; Lansalot, M. Effect of the pH on the RAFT Polymerization of Acrylic Acid in Water. Application to the Synthesis of Poly(acrylic acid)-Stabilized Polystyrene Particles by RAFT Emulsion Polymerization. *Macromolecules* **2013**, *46*, 6013–6023.
- (106) Jones, E. R.; Semsarilar, M.; Wyman, P.; Boerakker, M.; Armes, S. P. Addition of Water to an Alcoholic RAFT PISA Formulation Leads to Faster Kinetics but Limits the Evolution of Copolymer Morphology. *Polym. Chem.* **2016**, *7*, 851–859.
- (107) Chaduc, I.; Zhang, W.; Rieger, J.; Lansalot, M.; D'Agosto, F.; Charleux, B. Amphiphilic Block Copolymers from a Direct and One-Pot RAFT Synthesis in Water. *Macromol. Rapid Commun.* **2011**, *32*, 1270–1276.
- (108) Zhou, W.; Qu, Q.; Yu, W.; An, Z. Single Monomer for Multiple Tasks: Polymerization Induced Self-Assembly, Functionalization and Cross-Linking, and Nanoparticle Loading. *ACS Macro Lett.* **2014**, *3*, 1220–1224.
- (109) Lacík, I.; Učňová, L.; Kukučková, S.; Buback, M.; Hesse, P.; Beuermann, S. Propagation Rate Coefficient of Free-Radical Polymerization of Partially and Fully Ionized Methacrylic Acid in Aqueous Solution. *Macromolecules* **2009**, *42*, 7753–7761.
- (110) Stach, M.; Lacík, I.; Chorvát, D.; Buback, M.; Hesse, P.; Hutchinson, R. A.; Tang, L.; Chorvát, D., Jr.; Buback, M. Propagation Rate Coefficient for Radical Polymerization of *N*-Vinyl Pyrrolidone in Aqueous Solution Obtained by PLP-SEC. *Macromolecules* **2008**, *41*, 5174–5185.
- (111) Zhou, W.; Qu, Q.; Xu, Y.; An, Z. Aqueous Polymerization-Induced Self-Assembly for the Synthesis of Ketone-Functionalized Nano-Objects with Low Polydispersity. *ACS Macro Lett.* **2015**, *4*, 495–499.
- (112) Sugihara, S.; Armes, S. P.; Blanazs, A.; Lewis, A. L. Non-Spherical Morphologies from Cross-Linked Biomimetic Diblock Copolymers Using RAFT Aqueous Dispersion Polymerization. *Soft Matter* **2011**, *7*, 10787–10793.
- (113) Williams, M.; Penfold, N. J. W.; Armes, S. P. Cationic and Reactive Primary Amine-Stabilised Nanoparticles via RAFT Aqueous Dispersion Polymerisation. *Polym. Chem.* **2016**, *7*, 384–393.
- (114) Binauld, S.; Delafresnaye, L.; Charleux, B.; D'Agosto, F.; Lansalot, M. Emulsion Polymerization of Vinyl Acetate in the Presence of Different Hydrophilic Polymers Obtained by RAFT/MADIX. *Macromolecules* **2014**, *47*, 3461–3472.
- (115) Ning, Y.; Fielding, L. A.; Andrews, T. S.; Grownay, D.; Armes, S. P. Sulfate-Based Anionic Diblock Copolymer Nanoparticles for Efficient Occlusion within Zinc Oxide. *Nanoscale* **2015**, *7*, 6691–6702.

- (116) Chaduc, I.; Girod, M.; Antoine, R.; Charleux, B.; D'Agosto, F.; Lansalot, M. Batch Emulsion Polymerization Mediated by Poly-(methacrylic acid) macroRAFT Agents: One-Pot Synthesis of Self-Stabilized Particles. *Macromolecules* **2012**, *45*, 5881–5893.
- (117) St Thomas, C.; Guerrero-Santos, R.; D'Agosto, F. Alkoxy-amine-Functionalized Latex Nanoparticles through RAFT Polymerization-Induced Self-Assembly in Water. *Polym. Chem.* **2015**, *6*, 5405–5413.
- (118) Carlsson, L.; Fall, A.; Chaduc, I.; Wagberg, L.; Charleux, B.; Malmstrom, E.; D'Agosto, F.; Lansalot, M.; Carlmark, A. Modification of Cellulose Model Surfaces by Cationic Polymer Latexes Prepared by RAFT-Mediated Surfactant-Free Emulsion Polymerization. *Polym. Chem.* **2014**, *5*, 6076–6086.
- (119) Binks, B. P. Particles as Surfactants—Similarities and Differences. *Curr. Opin. Colloid Interface Sci.* **2002**, *7*, 21–41.
- (120) Thompson, K. L.; Mable, C. J.; Cockram, A.; Warren, N. J.; Cunningham, V. J.; Jones, E. R.; Verber, R.; Armes, S. P. Are Block Copolymer Worms More Effective Pickering Emulsifiers than Block Copolymer Spheres? *Soft Matter* **2014**, *10*, 8615–8626.
- (121) Thompson, K. L.; Fielding, L. A.; Mykhaylyk, O. O.; Lane, J. A.; Derry, M. J.; Armes, S. P. Vermicious Thermo-Responsive Pickering Emulsifiers. *Chem. Sci.* **2015**, *6*, 4207–4214.
- (122) Thompson, K. L.; Mable, C. J.; Lane, J. A.; Derry, M. J.; Fielding, L. A.; Armes, S. P. Preparation of Pickering Double Emulsions Using Block Copolymer Worms. *Langmuir* **2015**, *31*, 4137–4144.
- (123) Blanazs, A.; Verber, R.; Mykhaylyk, O. O.; Ryan, A. J.; Heath, J. Z.; Douglas, C. W. I.; Armes, S. P. Sterilizable Gels from Thermo-responsive Block Copolymer Worms. *J. Am. Chem. Soc.* **2012**, *134*, 9741–9748.
- (124) Verber, R.; Blanazs, A.; Armes, S. P. Rheological Studies of Thermo-Responsive Diblock Copolymer Worm Gels. *Soft Matter* **2012**, *8*, 9915–9922.
- (125) Pei, Y.; Thurairajah, L.; Sugita, O. R.; Lowe, A. B. RAFT Dispersion Polymerization in Nonpolar Media: Polymerization of 3-Phenylpropyl Methacrylate in *n*-Tetradecane with Poly(stearyl methacrylate) Homopolymers as Macro Chain Transfer Agents. *Macromolecules* **2015**, *48*, 236–244.
- (126) Pei, Y.; Dharsana, N. C.; Hensbergen, J. A.; Van Burford, R. P.; Roth, P. J.; Lowe, A. B. RAFT Dispersion Polymerization of 3-Phenylpropyl Methacrylate with Poly[2-(dimethylamino)ethyl methacrylate] Macro-CTAs in Ethanol and Associated Thermoreversible Polymorphism. *Soft Matter* **2014**, *10*, 5787–5796.
- (127) Liu, G.; Qiu, Q.; An, Z. Development of Thermosensitive Copolymers of Poly(2-methoxyethyl acrylate-co-poly(ethylene glycol methyl ether acrylate) and Their Nanogels Synthesized by RAFT Dispersion Polymerization in Water. *Polym. Chem.* **2012**, *3*, 504–513.
- (128) Liu, G.; Qiu, Q.; Shen, W.; An, Z. Aqueous Dispersion Polymerization of 2-Methoxyethyl Acrylate for the Synthesis of Biocompatible Nanoparticles Using a Hydrophilic RAFT Polymer and a Redox Initiator. *Macromolecules* **2011**, *44*, 5237–5245.
- (129) Shen, W.; Chang, Y.; Liu, G.; Wang, H.; Cao, A.; An, Z. Biocompatible, Antifouling, and Thermosensitive Core-Shell Nanogels Synthesized by RAFT Aqueous Dispersion Polymerization. *Macromolecules* **2011**, *44*, 2524–2530.
- (130) Hou, L.; Ma, K.; An, Z.; Wu, P. Exploring the Volume Phase Transition Behavior of POEGA- and PNIPAM-Based Core-Shell Nanogels from Infrared-Spectral Insights. *Macromolecules* **2014**, *47*, 1144–1154.
- (131) Charleux, B.; Alaimo, D.; Je, C.; Rieger, J. Pegylated Thermally Responsive Block Copolymer Micelles and Nanogels via In Situ RAFT Aqueous Dispersion Polymerization. *J. Polym. Sci., Part A: Polym. Chem.* **2009**, *47*, 2373–2390.
- (132) Jia, Z.; Bobrin, V. A.; Truong, N. P.; Gillard, M.; Monteiro, M. J. Multifunctional Nanoworms and Nanorods through a One-Step Aqueous Dispersion Polymerization. *J. Am. Chem. Soc.* **2014**, *136*, 5824–5827.
- (133) Chen, X.; Prowse, A. B. J.; Jia, Z.; Tellier, H.; Munro, T. P.; Gray, P. P.; Monteiro, M. J. Thermo-responsive Worms for Expansion and Release of Human Embryonic Stem Cells. *Biomacromolecules* **2014**, *15*, 844–855.
- (134) Truong, N. P.; Whittaker, M. R.; Anastasaki, A.; Haddleton, D. M.; Quinn, J. F.; Davis, T. P. Facile Production of Nanoaggregates with Tuneable Morphologies from Thermo-responsive P(DEGMA-co-HPMA). *Polym. Chem.* **2016**, *7*, 430–446.
- (135) Lovett, J. R.; Warren, N. J.; Ratcliffe, L. P. D.; Kocik, M. K.; Armes, S. P. pH-Responsive Non-Ionic Diblock Copolymers: Ionization of Carboxylic Acid End-Groups Induces an Order-Order Morphological Transition. *Angew. Chem.* **2015**, *127*, 1295–1299.
- (136) Penfold, N. J. W.; Lovett, J. R.; Warren, N. J.; Verstraete, P.; Smets, J.; Armes, S. P. pH-Responsive Non-Ionic Diblock Copolymers: Protonation of a Morpholine End-Group Induces an Order-Order Transition. *Polym. Chem.* **2016**, *7*, 79–88.
- (137) Dong, S.; Zhao, W.; Lucien, F. P.; Perrier, S.; Zetterlund, P. B. Polymerization Induced Self-Assembly: Tuning of Nano-Object Morphology by Use of CO<sub>2</sub>. *Polym. Chem.* **2015**, *6*, 2249–2254.
- (138) *Polymer Handbook*; Bandrup, J., Immergut, E. H., Eds.; Wiley-Interscience: 1975.
- (139) Ratcliffe, L. P. D.; McKenzie, B. E.; Le Bouëdec, G. M. D.; Williams, C. N.; Brown, S. L.; Armes, S. P. Polymerization-Induced Self-Assembly of All-Acrylic Diblock Copolymers via RAFT Dispersion Polymerization in Alkanes. *Macromolecules* **2015**, *48*, 8594–8607.
- (140) Warren, N. J.; Mykhaylyk, O. O.; Ryan, A. J.; Williams, M.; Doussineau, T.; Dugourd, P.; Antoine, R.; Portale, G.; Armes, S. P. Testing the Vesicular Morphology to Destruction: Birth and Death of Diblock Copolymer Vesicles Prepared via Polymerization-Induced Self-Assembly. *J. Am. Chem. Soc.* **2015**, *137*, 1929–1937.
- (141) Hedir, G. G.; Pitto-Barry, A.; Dove, A. P.; O'Reilly, R. K. Amphiphilic Block Copolymer Self-Assemblies of Poly(NVP)-*b*-poly(MDO-co-vinyl esters): Tunable Dimensions and Functionalities. *J. Polym. Sci., Part A: Polym. Chem.* **2015**, *53*, 2699–2710.
- (142) Doncom, K. E. B.; Willcock, H.; Lu, A.; McKenzie, B. E.; Kirby, N.; O'Reilly, R. K. Complementary Light Scattering and Synchrotron Small-Angle X-Ray Scattering Studies of the Micelle-to-Unimer Transition of Polysulfobetaines. *Soft Matter* **2015**, *11*, 3666–3676.
- (143) Jones, E. R.; Mykhaylyk, O. O.; Semsarilar, M.; Boerakker, M.; Wyman, P.; Armes, S. P. How Do Spherical Diblock Copolymer Nanoparticles Grow during RAFT Alcoholic Dispersion Polymerization? *Macromolecules* **2016**, *49*, 172–181.
- (144) Cunningham, V.; Ratcliffe, L.; Blanazs, A.; Warren, N. J.; Smith, A. J.; Mykhaylyk, O. O.; Armes, S. Tuning the Critical Gelation Temperature of Thermo-Responsive Diblock Copolymer Worm Gels. *Polym. Chem.* **2014**, *5*, 6307–6317.
- (145) Kocik, M. K.; Mykhaylyk, O. O.; Armes, S. P. Aqueous Worm Gels Can Be Reconstituted from Freeze-Dried Diblock Copolymer Powder. *Soft Matter* **2014**, *10*, 3984–3992.
- (146) Perrier, S.; Takolpuckdee, P.; Mars, C. A. Reversible Addition-Fragmentation Chain Transfer Polymerization: End Group Modification for Functionalized Polymers and Chain Transfer Agent Recovery. *Macromolecules* **2005**, *38*, 2033–2036.
- (147) Willcock, H.; O'Reilly, R. K. End Group Removal and Modification of RAFT Polymers. *Polym. Chem.* **2010**, *1*, 149–157.
- (148) Moad, G.; Rizzardo, E.; Thang, S. H. End-Functional Polymers, Thiocarbonylthio Group Removal/Transformation and Reversible Addition-Fragmentation-Chain Transfer (RAFT) Polymerization. *Polym. Int.* **2011**, *60*, 9–25.
- (149) Matioszek, D.; Dufils, P.; Vinas, J.; Destarac, M. Selective and Quantitative Oxidation of Xanthate End-Groups of RAFT Poly(*n*-butyl acrylate) Latexes by Ozonolysis. *Macromol. Rapid Commun.* **2015**, *36*, 1354–1361.
- (150) Ladmiraal, V.; Semsarilar, M.; Canton, I.; Armes, S. P. Polymerization-Induced Self-Assembly of Galactose-Functionalized Biocompatible Diblock Copolymers for Intracellular Delivery. *J. Am. Chem. Soc.* **2013**, *135*, 13574–13581.
- (151) Karagoz, B.; Yeow, J.; Esser, L.; Prakash, S. M.; Kuchel, R. P.; Davis, T. P.; Boyer, C. An Efficient and Highly Versatile Synthetic



Route to Prepare Iron Oxide Nanoparticles/Nanocomposites with Tunable Morphologies. *Langmuir* **2014**, *30*, 10493–10502.

(152) Ladmiral, V.; Charlot, A.; Semsarilar, M.; Armes, S. P. Synthesis and Characterization of Poly(amino acid methacrylate)-Stabilized Diblock Copolymer Nano-Objects. *Polym. Chem.* **2015**, *6*, 1805–1816.

(153) Bryztwa, A. J.; Johnson, J. Scaled Production of RAFT CTA—a STAR Performer. *Polym. Prepr. Am. Chem. Soc. Div. Polym. Chem.* **2011**, *52*, 533–534.

(154) Moad, G.; Rizzardo, E.; Thang, S. H. RAFT Polymerization and Some of Its Applications. *Chem. Asian J.* **2013**, *8*, 1634–1644.

(155) Percec, V.; Guliasvili, T.; Ladislav, J. S.; Wistrand, A.; Stjernedahl, A.; Sienkowska, M. J.; Monteiro, M. J.; Sahoo, S. Ultrafast Synthesis of Ultrahigh Molar Mass Polymers by Metal-Catalyzed Living Radical Polymerization of Acrylates, Methacrylates, and Vinyl Chloride Mediated by SET at 25 °C. *J. Am. Chem. Soc.* **2006**, *128*, 14156–14165.

(156) Nguyen, N. H.; Rosen, B. M.; Jiang, X.; Fleischmann, S.; Percec, V. New Efficient Reaction Media for SET-LRP Produced from Binary Mixtures of Organic Solvents and H<sub>2</sub>O. *J. Polym. Sci., Part A: Polym. Chem.* **2009**, *47*, 5577–5590.

(157) Whittaker, M. R.; Urbani, C. N.; Monteiro, M. J. Synthesis of Linear and 4-Arm Star Block Copolymers of Poly(methyl acrylate)-*b*-solketal acrylate by SET-LRP at 25 °C. *J. Polym. Sci., Part A: Polym. Chem.* **2008**, *46*, 6346–6357.

(158) Lligadas, G.; Percec, V. Ultrafast SET-LRP of Methyl Acrylate at 25 °C in Alcohols. *J. Polym. Sci., Part A: Polym. Chem.* **2008**, *46*, 2745–2754.

(159) Monge, S.; Darcos, V.; Haddleton, D. M. Effect of DMSO Used as Solvent in Copper Mediated Living Radical Polymerization. *J. Polym. Sci., Part A: Polym. Chem.* **2004**, *42*, 6299–6308.

(160) Bell, C. A.; Whittaker, M. R.; Gahan, L. R.; Monteiro, M. J. Outer-Sphere Electron Transfer Metal-Catalyzed Polymerization of Styrene Using a Macrocyclic Ligand CRAIG. *J. Polym. Sci., Part A: Polym. Chem.* **2008**, *46*, 146–154.

(161) Percec, V.; Popov, A. V.; Ramirez-Castillo, E.; Monteiro, M.; Barboiu, B.; Weichold, O.; Asandei, A. D.; Mitchell, C. M. Aqueous Room Temperature Metal-Catalyzed Living Radical Polymerization of Vinyl Chloride. *J. Am. Chem. Soc.* **2002**, *124*, 4940–4941.

(162) Gu, L.; Shen, Z.; Feng, C.; Li, Y.; Lu, G.; Huang, X. Synthesis of Double Hydrophilic Graft Copolymer Containing Poly(ethylene glycol) and Poly(methacrylic acid) Side Chains via Successive ATRP. *J. Polym. Sci., Part A: Polym. Chem.* **2008**, *46*, 4056–4069.

(163) Feng, C.; Shen, Z.; Gu, L.; Zhang, S.; Li, L.; Lu, G.; Huang, X. Synthesis and Characterization of PNIPAM-*b*-(PEA-*g*-PDEA) Double Hydrophilic Graft Copolymer. *J. Polym. Sci., Part A: Polym. Chem.* **2008**, *46*, 5638–5651.

(164) Feng, C.; Shen, Z.; Li, Y.; Gu, L.; Zhang, Y.; Lu, G.; Huang, X. PNIPAM-*b*-(PEA-*g*-PDMAEA) Double-Hydrophilic Graft Copolymer: Synthesis and Its Application for Preparation of Gold Nanoparticles in Aqueous Media. *J. Polym. Sci., Part A: Polym. Chem.* **2009**, *47*, 1811–1824.

(165) Percec, V.; Grigoras, C. Catalytic Effect of Ionic Liquids in the Cu<sub>2</sub>O/2,2'-Bipyridine Catalyzed Living Radical Polymerization of Methyl Methacrylate Initiated with Arenesulfonyl Chlorides. *J. Polym. Sci., Part A: Polym. Chem.* **2005**, *43*, 5609–5619.

(166) Wang, W.; Zhang, Z.; Zhu, J.; Zhou, N.; Zhu, X. Single Electron Transfer-Living Radical Polymerization of Methyl Methacrylate in Fluoroalcohol: Dual Control Over Molecular Weight and Tacticity. *J. Polym. Sci., Part A: Polym. Chem.* **2009**, *47*, 6316–6327.

(167) Kapishon, V.; Whitney, R. A.; Champagne, P.; Cunningham, M. F.; Neufeld, R. J. Polymerization Induced Self-Assembly of Alginate Based Amphiphilic Graft Copolymers Synthesized by Single Electron Transfer Living Radical Polymerization. *Biomacromolecules* **2015**, *16*, 2040–2048.

(168) Yamago, S.; Iida, K.; Yoshida, J. I. Organotellurium Compounds as Novel Initiators for Controlled/Living Radical Polymerizations. Synthesis of Functionalized Polystyrenes and End-Group Modifications. *J. Am. Chem. Soc.* **2002**, *124*, 2874–2875.

(169) Yamago, S. Precision Polymer Synthesis by Degenerative Transfer Controlled/Living Radical Polymerization Using Organotellurium, Organostibine, and Organobismuthine Chain-Transfer Agents. *Chem. Rev.* **2009**, *109*, 5051–5068.

(170) Okubo, M.; Sugihara, Y.; Kitayama, Y.; Kagawa, Y.; Minami, H. Emulsifier-Free, Organotellurium-Mediated Living Radical Emulsion Polymerization of Butyl Acrylate. *Macromolecules* **2009**, *42*, 1979–1984.

(171) Kitayama, Y.; Kishida, K.; Minami, H.; Okubo, M. Preparation of Poly(*n*-butyl acrylate)-*b*-polystyrene Particles by Emulsifier-Free, Organotellurium-Mediated Living Radical Emulsion Polymerization (Emulsion TERP). *J. Polym. Sci., Part A: Polym. Chem.* **2012**, *50*, 1991–1996.

(172) Tan, J.; Sun, H.; Yu, M.; Sumerlin, B. S.; Zhang, L. Photo-PISA: Shedding Light on Polymerization-Induced Self-Assembly. *ACS Macro Lett.* **2015**, *4*, 1249–1253.

(173) Mable, C. J.; Gibson, R. R.; Prévost, S.; McKenzie, B. E.; Mykhaylyk, O. O.; Armes, S. P. Loading of Silica Nanoparticles in Block Copolymer Vesicles during Polymerization-Induced Self-Assembly: Encapsulation Efficiency and Thermally-Triggered Release. *J. Am. Chem. Soc.* **2015**, *137*, 16098–16108.

(174) Canton, I.; Massignani, M.; Patikarnmonthon, N.; Chierico, L.; Robertson, J.; Renshaw, S. A.; Warren, N. J.; Madsen, J. P.; Armes, S. P.; Lewis, A. L.; et al. Fully Synthetic Polymer Vesicles for Intracellular Delivery of Antibodies in Live Cells. *FASEB J.* **2013**, *27*, 98–108.

(175) Tanner, P.; Baumann, P.; Enea, R.; Onaca, O.; Palivan, C.; Meier, W. Polymeric Vesicles: From Drug Carriers to Nanoreactors and Artificial Organelles. *Acc. Chem. Res.* **2011**, *44*, 1039–1049.

(176) Karagoz, B.; Boyer, C.; Davis, T. P. Simultaneous Polymerization-Induced Self-Assembly (PISA) and Guest Molecule Encapsulation. *Macromol. Rapid Commun.* **2014**, *35*, 417–421.

(177) Moad, G.; Rizzardo, E.; Thang, S. H. Radical Addition–Fragmentation Chemistry in Polymer Synthesis. *Polymer* **2008**, *49*, 1079–1131.

(178) An, Z.; Shi, Q.; Tang, W.; Tsung, C.; Hawker, C. J.; Stucky, G. D. Facile RAFT Precipitation Polymerization for the Microwave-Assisted Synthesis of Well-Defined, Double Hydrophilic Block Copolymers and Nanostructured Hydrogels. *J. Am. Chem. Soc.* **2007**, *129*, 14493–14499.

(179) Pei, Y.; Lowe, A. B. Polymerization-Induced Self-Assembly: Ethanolic RAFT Dispersion Polymerization of 2-Phenylethyl Methacrylate. *Polym. Chem.* **2014**, *5*, 2342–2351.

(180) Figg, C. A.; Simula, A.; Gebre, K. A.; Tucker, B. S.; Haddleton, D. M.; Sumerlin, B. S. Polymerization-Induced Thermal Self-Assembly (PITSA). *Chem. Sci.* **2015**, *6*, 1230–1236.

(181) Xiao, X.; He, S.; Dan, M.; Su, Y.; Huo, F.; Zhang, W. Brush Macro-RAFT Agent Mediated Dispersion Polymerization of Styrene in the Alcohol/Water Mixture. *J. Polym. Sci., Part A: Polym. Chem.* **2013**, *51*, 3177–3190.

(182) Canton, I.; Warren, N. J.; Chahal, A.; Amps, K.; Wood, A.; Weightman, R.; Wang, E.; Moore, H.; Armes, S. P. Mucin-Inspired Thermoresponsive Synthetic Hydrogels Induce Stasis in Human Pluripotent Stem Cells and Human Embryos. *ACS Cent. Sci.* **2016**, *2*, 65–74.

(183) Warren, N. J.; Rosselgong, J.; Madsen, J.; Armes, S. P. Disulfide-Functionalized Diblock Copolymer Worm Gels. *Biomacromolecules* **2015**, *16*, 2514–2521.

(184) Simon, K. A.; Warren, N. J.; Mosadegh, B.; Mohammady, M. R.; Whitesides, G. M.; Armes, S. P. Disulfide-Based Diblock Copolymer Worm Gels: A Wholly-Synthetic Thermoreversible 3D Matrix for Sheet-Based Cultures. *Biomacromolecules* **2015**, *16*, 3952–3958.

(185) Derda, R.; Laromaine, A.; Mammoto, A.; Tang, S. K. Y.; Mammoto, T.; Ingber, D. E.; Whitesides, G. M. Paper-Supported 3D Cell Culture for Tissue-Based Bioassays. *Proc. Natl. Acad. Sci. U. S. A.* **2009**, *106*, 18457–18462.

(186) Chambon, P.; Blanazs, A.; Battaglia, G.; Armes, S. P. How Does Cross-Linking Affect the Stability of Block Copolymer Vesicles in the Presence of Surfactant? *Langmuir* **2012**, *28*, 1196–1205.



(187) Zhang, W.; Charleux, B.; Cassagnau, P. Dynamic Behavior of Crosslinked Amphiphilic Block Copolymer Nanofibers Dispersed in Liquid Poly(ethylene oxide) below and above Their Glass Transition Temperature. *Soft Matter* **2013**, *9*, 2197–2205.

(188) Zhang, X.; Cardozo, A. F.; Chen, S.; Zhang, W.; Julcour, C.; Lansalot, M.; Blanco, J.-F.; Gayet, F.; Delmas, H.; Charleux, B.; Manoury, E.; D'Agosto, F.; Poli, R. Core–Shell Nanoreactors for Efficient Aqueous Biphasic Catalysis. *Chem. Eur. J.* **2014**, *20*, 15505–15517.

(189) Thompson, K. L.; Chambon, P.; Verber, R.; Armes, S. P. Can Polymersomes Form Colloidosomes? *J. Am. Chem. Soc.* **2012**, *134*, 12450–12453.

(190) Tyndall, J. On the Action of Rays of High Refrangibility upon Gaseous Matter. *Philos. Trans. R. Soc. London* **1870**, *160*, 333–365.

(191) Ratcliffe, L. P. D.; Blanazs, A.; Williams, C. N.; Brown, S. L.; Armes, S. P. RAFT Polymerization of Hydroxy-Functional Methacrylic Monomers under Heterogeneous Conditions: Effect of Varying the Core-Forming Block. *Polym. Chem.* **2014**, *5*, 3643–3655.

(192) Schmelz, J.; Schedl, A. E.; Steinlein, C.; Manners, I.; Schmalz, H. Length Control and Block-Type Architectures in Worm-like Micelles with Polyethylene Cores. *J. Am. Chem. Soc.* **2012**, *134*, 14217–14225.

(193) Bobrin, V. A.; Monteiro, M. J. Temperature-Directed Self-Assembly of Multifunctional Polymeric Tadpoles. *J. Am. Chem. Soc.* **2015**, *137*, 15652–15655.

(194) Zhulina, E. B.; Adam, M.; Larue, I.; Sheiko, S. S.; Rubinstein, M. Diblock Copolymer Micelles in a Dilute Solution. *Macromolecules* **2005**, *38*, 5330–5351.

(195) Thompson, K. L.; Lane, J. A.; Derry, M. J.; Armes, S. P. Non-Aqueous Isorefractive Pickering Emulsions. *Langmuir* **2015**, *31*, 4373–4376.

(196) Semsarilar, M.; Jones, E. R.; Armes, S. P. Comparison of Pseudo-Living Character of RAFT Polymerizations Conducted under Homogeneous and Heterogeneous Conditions. *Polym. Chem.* **2014**, *5*, 195–203.

(197) Zheng, R.; Liu, G.; Devlin, M.; Hux, K.; Jao, T. Friction Reduction of Lubricant Base Oil by Micelles and Crosslinked Micelles of Block Copolymers. *Tribol. Trans.* **2009**, *53*, 97–107.

(198) Cardozo, A. F.; Julcour, C.; Barthe, L.; Blanco, J.-F.; Chen, S.; Gayet, F.; Manoury, E.; Zhang, X.; Lansalot, M.; Charleux, B.; D'Agosto, F.; Poli, H.; Delmas, H. Aqueous Phase Homogeneous Catalysis Using Core–Shell Nanoreactors: Application to Rhodium-Catalyzed Hydroformylation of 1-Octene. *J. Catal.* **2015**, *324*, 1–8.

(199) Nguyen, D.; Zondanos, H. S.; Farrugia, J. M.; Serelis, A. K.; Such, C. H.; Hawkett, B. S. Pigment Encapsulation by Emulsion Polymerization Using Macro-RAFT Copolymers. *Langmuir* **2008**, *24*, 2140–2150.

(200) Mitchell, D. E.; Lovett, J. R.; Armes, S. P.; Gibson, M. I. Combining Biomimetic Block Copolymer Worms with an Ice-Inhibiting Polymer for the Solvent-Free Cryopreservation of Red Blood Cells. *Angew. Chem. Int. Ed.* **2016**, *55*, 2801–2804.

(201) Guo, L.; Jiang, Y.; Qiu, T.; Meng, Y.; Li, X. One-Pot Synthesis of Poly(methacrylic acid)-*b*-poly(2,2,2-trifluoroethyl methacrylate) Diblock Copolymers via RAFT Polymerization. *Polymer* **2014**, *55*, 4601–4610.

(202) Rieger, J.; Osterwinter, G.; Bui, C.; Stoffelbach, F.; Charleux, B. Surfactant-Free Controlled/Living Radical Emulsion (Co)-polymerization of *n*-Butyl Acrylate and Methyl Methacrylate via RAFT Using Amphiphilic Polyethylene Oxide-Based Trithiocarbonate Chain Transfer Agents. *Macromolecules* **2009**, *42*, 5518–5525.

(203) Hanisch, A.; Yang, P.; Kulak, A. N.; Fielding, L. A.; Meldrum, F. C.; Armes, S. P. Phosphonic Acid-Functionalized Diblock Copolymer Nano-Objects via Polymerization-Induced Self-Assembly: Synthesis, Characterization and Occlusion into Calcite Crystals. *Macromolecules* **2016**, *49*, 192–204.

(204) Jiang, Y.; Xu, N.; Han, J.; Yu, Q.; Guo, L.; Gao, P.; Lu, X.; Cai, Y. The Direct Synthesis of Interface-Decorated Reactive Block Copolymer Nanoparticles via Polymerisation-Induced Self-Assembly. *Polym. Chem.* **2015**, *6*, 4955–4965.